

AD-A058 524

HUGHES RESEARCH LABS MALIBU CALIF  
ULTRA LOW LOSS COATINGS OF KCL LASER WINDOWS. (U)  
MAR 78 D ZUCCARO

F/G 11/3

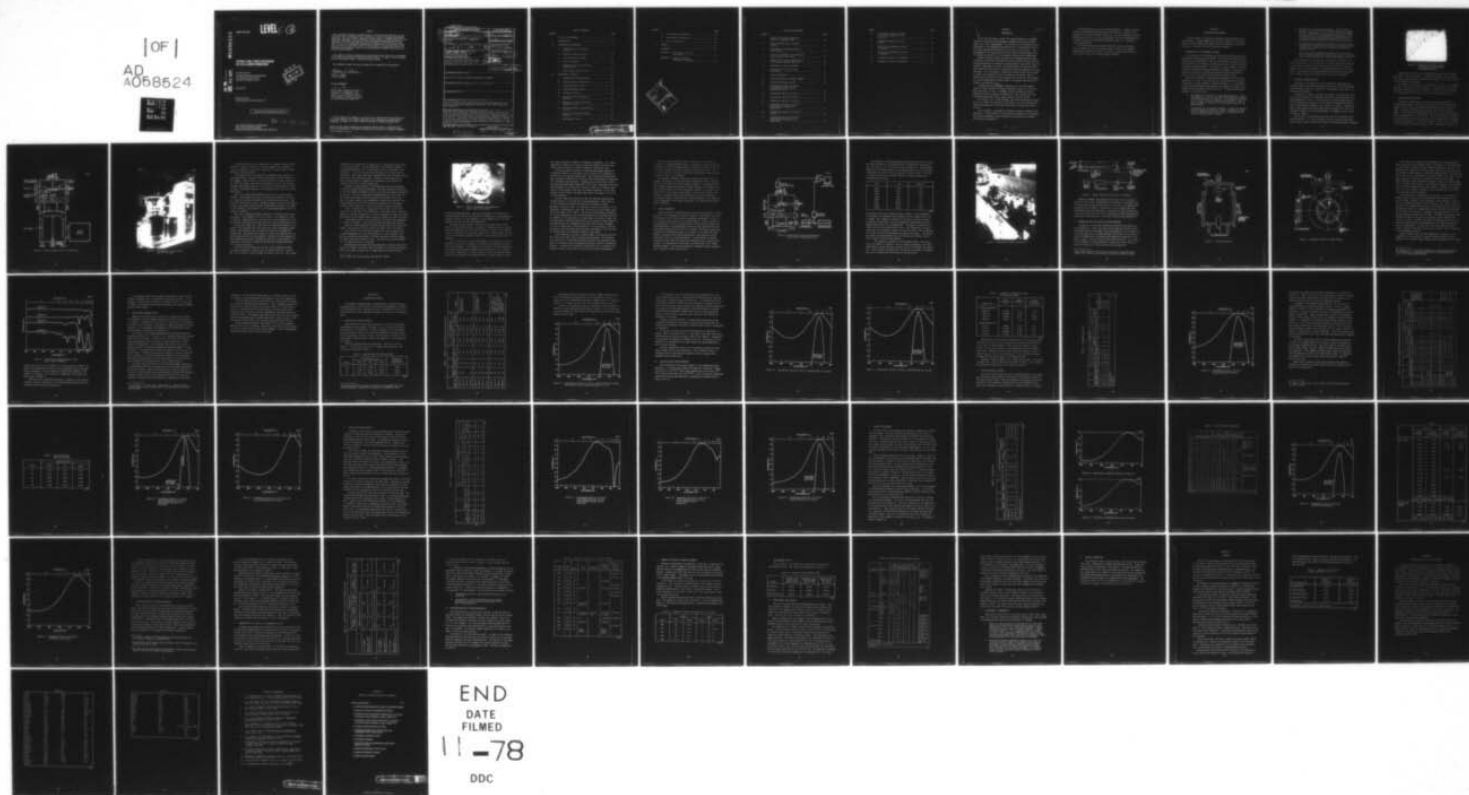
UNCLASSIFIED

AFML-TR-78-20

F33615-76-C-5319  
NL

[OF]

AD  
A058524





AD A 0 58 524

AFML-TR-78-20

LEVEL II

2  
NW

## ULTRA LOW LOSS COATINGS OF KCI LASER WINDOWS

DAVID ZUCCARO  
HUGHES RESEARCH LABORATORIES  
3011 MALIBU CANYON ROAD  
MALIBU, CALIFORNIA 90265

MARCH 1978

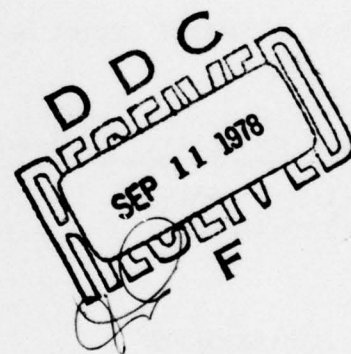
F33615-76-C-5319  
Final Report June 1976 to December 1977

Approved for public release; distribution unlimited.

78 15 08 076

AIR FORCE MATERIALS LABORATORY  
AIR FORCE SYSTEMS COMMAND  
WRIGHT-PATTERSON AIR FORCE BASE, OHIO 45433

AU NO. \_\_\_\_\_  
DDC FILE COPY



NOTICE

When Government drawings, specifications, or other data are used for any purpose other than in connection with a definitely related Government procurement operation, the United States Government thereby incurs no responsibility nor any obligation whatsoever; and the fact that the government may have formulated, furnished, or in any way supplied the said drawings, specifications, or other data, is not to be regarded by implication or otherwise as in any manner licensing the holder or any other person or corporation, or conveying any rights or permission to manufacture, use, or sell any patented invention that may in any way be related thereto.

This report has been reviewed by the Information Office (OI) and is releasable to the National Technical Information Service (NTIS). At NTIS, it will be available to the general public, including foreign nations.

This technical report has been reviewed and is approved for publication.

Melvin C Ohmer

MELVIN C. OHMER  
Project Engineer

FOR THE COMMANDER

William G. D. Frederick

WILLIAM G. D. FREDERICK, Chief  
Laser & Optical Materials Branch  
Electromagnetic Materials Division  
Air Force Materials Laboratory

"If your address has changed, if you wish to be removed from our mailing list, or if the addressee is no longer employed by your organization please notify AFML/LPO, W-PAFB, OH 45433 to help us maintain a current mailing list".

Copies of this report should not be returned unless return is required by security considerations, contractual obligations, or notice on a specific document.

UNCLASSIFIED

SECURITY CLASSIFICATION OF THIS PAGE (When Data Entered)

19 REPORT DOCUMENTATION PAGE		READ INSTRUCTIONS BEFORE COMPLETING FORM	
1. REPORT NUMBER	2. GOVT ACCESSION NO.	3. RECIPIENT'S CATALOG NUMBER	
AFML TR-78-28		Final rept.	
4. TITLE (and Subtitle)	5. TYPE OF REPORT & PERIOD COVERED		
ULTRA LOW LOSS COATINGS OF KCl LASER WINDOWS	1 Jun 76 - 31 Dec 77		
6. AUTHOR(s)		7. PERFORMING ORG. REPORT NUMBER	
D. Zuccaro			
8. CONTRACT OR GRANT NUMBER(s)		9. PROGRAM ELEMENT, PROJECT, TASK AREA & WORK UNIT NUMBER	
F33615-76-C-5319		317J-00-23	
10. PERFORMING ORGANIZATION NAME AND ADDRESS		11. REPORT DATE	
Hughes Aircraft Company Hughes Research Laboratories 3011 Malibu Canyon Road Malibu, California 90265		Mar 78	
12. CONTROLLING OFFICE NAME AND ADDRESS		13. NUMBER OF PAGES	
Air Force Materials Laboratory (LPO) Wright-Patterson AF Base, Ohio 45433		73	
14. MONITORING AGENCY NAME & ADDRESS (if different from Controlling Office)		15. SECURITY CLASS. (of this report)	
		Unclassified	
16. DISTRIBUTION STATEMENT (of this Report)		17. DISTRIBUTION STATEMENT (of the abstract entered in Block 20, if different from Report)	
Approved for public release; distribution unlimited.			
18. SUPPLEMENTARY NOTES			
19. KEY WORDS (Continue on reverse side if necessary and identify by block number)			
Optical coatings, As <sub>2</sub> S <sub>3</sub> , As <sub>2</sub> Se <sub>3</sub> , KCl, NaF, TlI, ZnSe materials, 9.27 μm AR coatings, Laser damage, Polycrystalline KCl, Surface finishing UHV deposition.			
20. ABSTRACT (Continue on reverse side if necessary and identify by block number)			
Low loss AR coatings were developed for polycrystalline KCl at 9.27 μm. Optical absorption losses of 0.03 to 0.09% per surface were achieved. The coatings were ZnSe/KCl/ZnSe, As <sub>2</sub> S <sub>3</sub> /KCl/As <sub>2</sub> S <sub>3</sub> , As <sub>2</sub> Se <sub>3</sub> /KCl/As <sub>2</sub> Se <sub>3</sub> , and TlI/KCl/TlI. Deposition under UHV conditions was essential to achieve the low coating absorption. Films containing either As <sub>2</sub> Se <sub>3</sub> or TlI had significantly higher absorption when deposited in the presence of water vapor of about 1 x 10 <sup>-8</sup> Torr.			

DD FORM 1 JAN 73 1473 EDITION OF 1 NOV 65 IS OBSOLETE

UNCLASSIFIED

SECURITY CLASSIFICATION OF THIS PAGE (When Data Entered)

172 600

78 15 08 076  
Gull

# TABLE OF CONTENTS

SECTION		PAGE
	LIST OF ILLUSTRATIONS . . . . .	5
I	INTRODUCTION . . . . .	7
II	APPARATUS AND PROCEDURES . . . . .	9
	A. Preparation of the Substrate Surfaces . . . . .	9
	B. Substrate Characterization . . . . .	10
	C. Coating Deposition System . . . . .	11
	D. Laser Calorimeter . . . . .	18
	E. Preparation and Purification of Film Materials . . . . .	22
	F. Laser Damage Threshold Tests . . . . .	27
III	DISCUSSION OF RESULTS . . . . .	29
	A. ZnSe/KCl/ZnSe Coating Results . . . . .	29
	B. As <sub>2</sub> S <sub>3</sub> /KCl/As <sub>2</sub> S <sub>3</sub> Coating Results . . . . .	32
	C. As <sub>2</sub> Se <sub>3</sub> /KCl/As <sub>2</sub> Se <sub>3</sub> Results . . . . .	35
	D. As <sub>2</sub> Se <sub>3</sub> /NaF/As <sub>2</sub> Se <sub>3</sub> Results . . . . .	43
	E. TlI/KCl/TlI Results . . . . .	48
	F. Polycrystalline KCl Substrate Materials . . . . .	55
	G. Comparison of 9.27 and 10.6 μm Absorption in KCl . . . . .	56
	H. Recrystallization in Polycrystalline KCl . . . . .	58
	I. Effects of Etching on Surface Flatness . . . . .	60
	J. Environmental Tests . . . . .	61



# LIST OF ILLUSTRATIONS

FIGURE		PAGE
1	Residue of polishing compound on surface of substrate 1288 . . . . .	11
2	Cross sectional view of the UHV system . . . . .	12
3	Photograph of the UHV system used in this study . . . . .	13
4	View of the Knudsen type evaporation sources used in this study . . . . .	16
5	System for the optical monitoring of film thickness during deposition . . . . .	19
6	Photograph of laser calorimeter . . . . .	21
7	Optical train of the CO <sub>2</sub> laser calorimeter . . . . .	22
8	Vacuum calorimeter . . . . .	23
9	Calorimeter mount for window samples . . . . .	24
10	Composite HRL As <sub>2</sub> Se <sub>3</sub> glasses . . . . .	26
11	Transmission spectra of 1272-2-1 which exhibits oxide related absorption at 9 μm . . . . .	31
12	Transmission spectra of 9-2-3-3 . . . . .	33
13	Transmission spectra of 1282-4-3 . . . . .	34
14	Transmission spectra of 9-12-5-4 . . . . .	37
15	Transmission spectra of 9-11-6-2 which exhibits strong 9 μm absorption . . . . .	41
16	Transmission spectra of 155-5-12-24-10-2 . . . . .	42
17	Transmission spectra of 9-10-7-1 which exhibits strong 13.6 μm absorption . . . . .	45

FIGURE		PAGE
18	Transmission spectra of 150-4-14-7-4 which exhibits 13.6 $\mu\text{m}$ absorption . . . . .	46
19	Transmission spectra of 174-5-30-9-1 . . . . .	47
20	Theoretical transmission spectra of design T1 . . . . .	50
21	Theoretical transmission spectra of design T2 . . . . .	50
22	Transmission spectra of 1992-18-4 . . . . .	52
23	Transmission spectra of 8E9-16-2 . . . . .	54

SECTION I  
INTRODUCTION

MICRO M

In the last few years, several low optical absorption 10.6  $\mu\text{m}$  AR coatings for KCl have been developed at Hughes Research Laboratories (HRL) and at other laboratories. The objective of this program was the development of 9.27  $\mu\text{m}$  AR coatings which have a film absorption loss of less than 0.01% and a reflection of less than 0.1% per surface. The achievement of the program objective will permit the development of a 9.27  $\mu\text{m}$  AR coating for a 32.5 cm diameter polycrystalline KCl window.

Because previous studies had shown that coatings deposited under ultra-high vacuum (UHV) conditions had lower absorption losses than did coatings deposited in conventional vacuum systems, the present study was limited to UHV-deposited films. Mass spectrometer analysis had shown that impurities were evolved occasionally during the evaporation of film materials. As a consequence, residual gas analysis (RGA) was performed to ensure that impurities were not present in the system. Also, if impurities were located in the film materials, either they were removed by reactive atmosphere processing (RAP) or techniques were developed to prepare clean material.

Although previous experience indicated that the major emphasis should be placed initially on films using ZnSe,  $\text{As}_2\text{S}_3$ , TlI,  $\text{ThF}_4$ , KCl,  $\text{BaF}_2$ , NaF,  $\text{CeF}_3$ , or  $\text{SrF}_2$ , a thorough literature search was made to determine the most promising film materials. The coatings that were studied included ZnSe,  $\text{As}_2\text{S}_3$ ,  $\text{As}_2\text{Se}_3$ , and TlI with KCl or NaF.

Five types of 9.27  $\mu\text{m}$  AR coatings, which had film absorption losses of 0.03 to 0.09%, were produced in this study. The 10.6  $\mu\text{m}$  absorption losses were measured in some cases and found to be about half that at 9.27  $\mu\text{m}$ .

In the program, a technique for substrate surface preparation was developed. It made possible the reproducible preparation of substrates that had low absorption, good flatness and parallelism, and freedom from surface contamination.

A UHV system was set up for the film deposition. A sample mounting system was developed that made possible the individual coating of both surfaces of the samples during a single run. We also developed efficient Knudsen-type sources for use in this program. The film thicknesses were accurately monitored on the sample surface by means of a transmitted light interferometer.

The coating absorption was determined with a vacuum calorimeter using a tunable  $\text{CO}_2$  laser as the power source. Most of the samples produced were submitted to AFML for focussed or broad beam testing (at 10.6 and 9.27  $\mu\text{m}$ ) of the cw laser damage threshold.

## SECTION II

### APPARATUS AND PROCEDURES

In this section, we discuss the apparatus and procedures used in this program. Although commercially available equipment is described briefly, special components designed under this program are described in detail. The same is true of operating procedures.

#### A. PREPARATION OF THE SUBSTRATE SURFACES

At the start of this program, polycrystalline KCl substrates were individually hand-ground and polished. This process was both expensive and difficult to standardize. Not only did changes in personnel result in variations in the substrate absorption, but even a single operator's production showed variations. As a result, it was necessary to develop a method for machine polishing substrates in batches. In addition to being very efficient, the method consistently produced high quality optical surfaces with good flatness and with parallel faces.

The process consists of grinding and polishing a batch of seven substrates at a time. The first step is to hand grind the substrates on SiC paper to obtain samples of uniform thickness. It is important to bevel the edges because sharp edges on the sample can break off and produce severe scratches on the KCl surface. The detailed polishing procedure is outlined below.

1. The samples are attached to a glass mandrel with wax. They are ground on a cast iron lap using 20  $\mu\text{m}$  loose grit abrasive with ethylene glycol as a vehicle. The grinding is continued until at least 0.1 mm is removed from the surface. This is done to ensure the removal of any deep damage caused by the hand grinding.
2. The surfaces are cleaned with propanol to remove the abrasive. Then the samples are ground on a glass lap using 9  $\mu\text{m}$  loose grit with ethylene glycol as a vehicle. Grinding proceeds until at least 0.05 mm is removed.

3. The surfaces are cleaned with propanol. Then the entire assembly is placed in concentrated HCl and etched for three minutes. The purpose of the etch is to remove all embedded polishing material and the damaged surface material. This step was found to be necessary because large particles of the grinding medium occasionally would be carried into the polishing step and produce severe scratches on the surface.
4. The substrates are polished on a Swiss Pitch lap with Linde A and propanediol for at least four hours. Following this the substrates are removed from the plate and ultrasonically cleaned in xylene.
5. The reverse side is ground and polished in the same manner. After the samples have been cleaned, they receive a very light buff on Polytex Supreme with Linde B and isopropyl alcohol.

After inspection of the surfaces, the samples are etched to stabilize the surfaces. They receive a 15 s etch in concentrated HCl and a 15 s rinse in isopropyl alcohol; then they are dried in an N<sub>2</sub> gas stream. Prior to this program, the substrates were dried in hot Freon vapor. This practice was discontinued because the Freon occasionally left a residue and because thermal shock could crack the sample.

#### B. SUBSTRATE CHARACTERIZATION

Following the polishing of the KCl substrates, the samples are inspected under a low power microscope (20 to 50 X), with a polariscope and with oblique light in a light box. The purpose of this step is to locate any large flaws.

If there are no flaws, the sample is etched. Following this step, it is again inspected in a light box, where any residual material on the surface appears as a film. In the early part of the program (when the final polishing step consisted of a hand buff on flannel with Linde A), these films sometimes appeared on the surfaces of the KCl. Examination under a high powered microscope (about 500 X) revealed this film to be composed of grains of the polishing medium. An example of such a film is shown in Figure 1.

Residue has not been observed since the use of the mechanical polishing technique. It is quite probable that the ultrasonic bath with xylene used to remove the wax also removes the residual polishing compound.

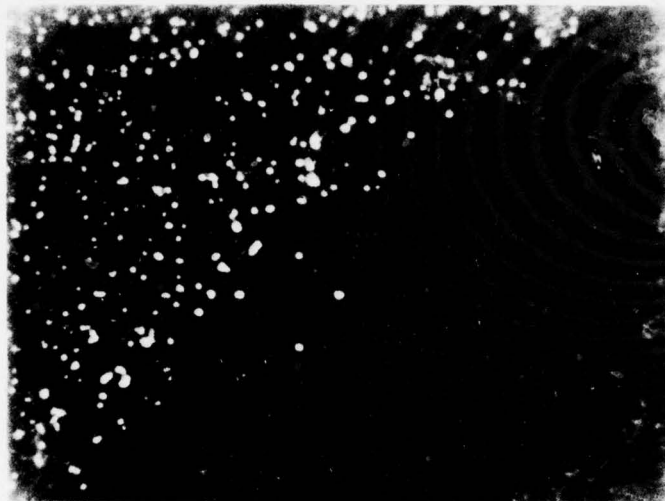


Figure 1. Residue of polishing compound on surface of substrate 1288 (160X magnification).

About 40% of the surfaces are inspected with dark field illumination, which accentuates surface contaminants and phase contrast microscopy which exposes surface and sub-surface damage, such as that caused by the grinding and polishing.

The substrate's absorption is determined at  $9.27\text{ }\mu\text{m}$  for all samples and also at  $10.6\text{ }\mu\text{m}$  for selected samples. The substrates are stored in individual holders that are contained in a plastic box. They are kept in a vacuum desiccator except for the periods when they are in use.

#### C. COATING DEPOSITION SYSTEM

The optical films produced in this program were deposited in an all metal UHV system. The vacuum system consists of a stainless-steel chamber, 46 cm in diameter and 100 cm in height, a 400 l/s diode ion pump, a titanium sublimation pump, and  $\text{LN}_2$  cooled zeolite sorption pumps. After evaluation under a  $200^\circ\text{C}$  bake-out for 36 hours, the system has a base pressure of  $2 \times 10^{-10}$  Torr. After the formation of deposits of film materials like  $\text{As}_2\text{S}_3$  and  $\text{As}_2\text{Se}_3$  on the interior walls, the base pressure, after bake-out, increases to about  $2 \times 10^{-9}$  Torr. A sectional view of the system is shown in Figure 2 and a photograph in Figure 3.

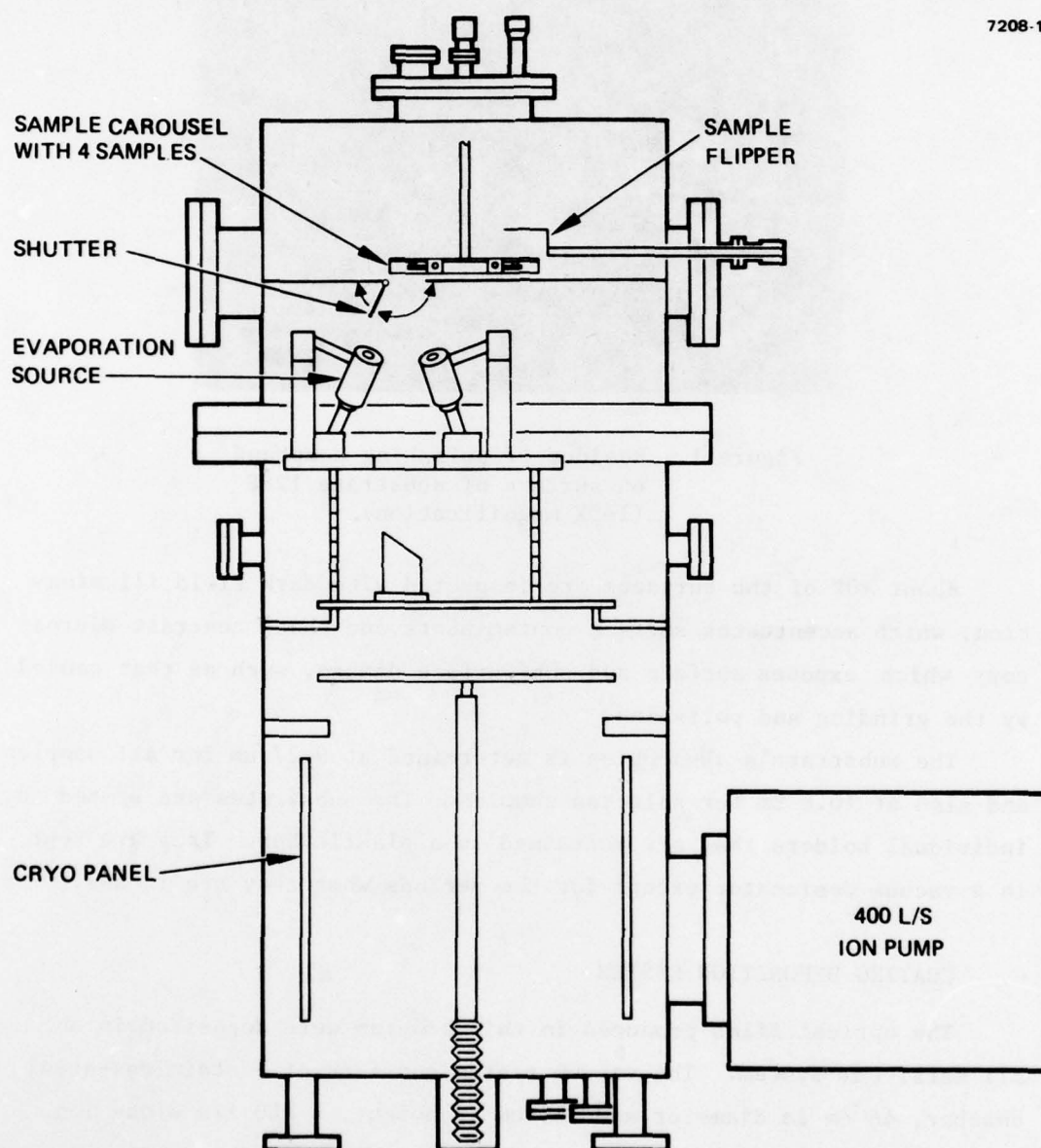


Figure 2. Cross sectional view of the UHV system.

M11750

7208-7

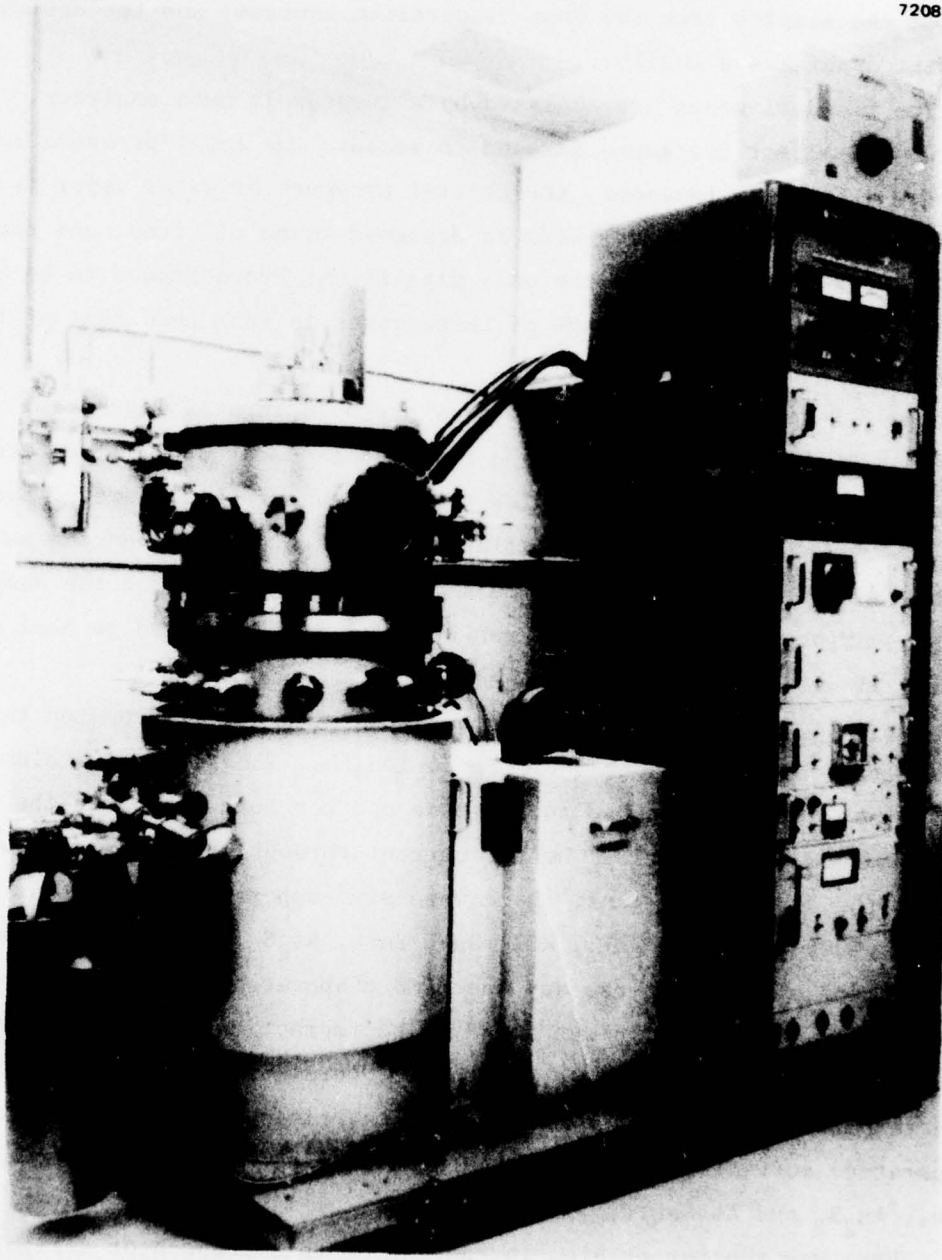


Figure 3. Photograph of the UHV system used in this study.

The major film deposition components are a sample carousel, which holds four samples; a flipper to turn the samples over; a shutter to isolate the samples from the four evaporation sources; and the optical deposition thickness monitor.

The residual gases are analyzed by a quadrupole mass analyzer. A nude Bayard-Alpert ion gauge is used to measure the total pressure in the chamber. After bake-out, the partial pressure of water vapor is in the  $10^{-11}$  Torr range. The system is designed to be oil free, and the residual gas analysis shows the only significant hydrocarbons to be  $\text{CH}_4$  and  $\text{C}_2\text{H}_6$ . The partial pressure of these gases is less than that of the water vapor.

The 3.8 cm diameter KCl substrates are held in stainless-steel holders. These holders slip into a four position carousel. The carousel rotates to position the samples over the evaporation sources. Samples are coated one at a time. A flipper is used to turn over the samples so that both surfaces can be coated without having to expose the sample to the atmosphere. The carousel can be electrically heated to heat the samples if desired.

The initial evaporator design consisted of a directly heated tantalum sleeve 1 cm in diameter and 5 cm in length. The sleeve was closed at the base. Leads attached to the base and top both supported the unit and conducted the electrical heater current through the evaporator walls.

In the first three runs, there were six evaporation sources in the system. They contained  $\text{ThF}_4$ , KCl, NaF, ZnSe,  $\text{As}_2\text{S}_3$ , and  $\text{As}_2\text{Se}_3$ , respectively. The plan was to use any specific evaporator to produce the desired film. This design was found to be impractical because the evaporation sources were too close together. Operation of one evaporator at high temperatures results in heating the material in other sources to a temperature sufficient to evaporate the high vapor pressure materials (i.e.,  $\text{As}_2\text{S}_3$  and  $\text{As}_2\text{Se}_3$ ).

There was another problem in the use of this evaporator design. The maximum temperature region was in the central portion of the unit due to the conduction losses through the leads at each end. This caused

problems in the evaporation of  $\text{As}_2\text{S}_3$  and  $\text{KCl}$ . When heated,  $\text{As}_2\text{S}_3$  forms a very viscous liquid. As the temperature is increased to achieve a reasonable evaporation rate, a vapor bubble forms in the center of the evaporator. It forces the cooler viscous  $\text{As}_2\text{S}_3$  out of the top of the evaporator. This causes very rapid changes in the vapor flux and creates problems in film thickness control. The  $\text{KCl}$  is evaporated from the hotter central region. Gradually  $\text{KCl}$  condenses at the mouth of the evaporator until it is nearly sealed off.

Because of these problems, a new evaporation source was designed. The interior dimensions were unchanged. The wall thickness was adjusted to have the highest resistance at the top and thus the highest temperature at the top. This was accomplished by adding material to the lower wall and serrating the upper part to increase the resistance at the top. Also, the upper conductor was redesigned to reduce the conduction loss. A three-layer heat shield of 0.01 mm thick tantalum foil was used to reduce the heat losses and to prevent heating of nearby evaporators.

Liners of either  $\text{SiO}_2$  or  $\text{Al}_2\text{O}_3$ , made in the shape of test tubes with 0.3 to 0.4 mm walls, were fabricated. These were used in the evaporators to contain the material. It was now possible to remove one sleeve and replace it with another without having to change the entire structure.

A new support structure was constructed that holds four evaporators. It is shown in Figure 4. The unit has proven dependable and versatile.

There is a single manually activated shutter located just below the sample. The shutter is used to control the vapor flux to the sample.

A key factor in the successful deposition of an AR coating is the accurate determination of the film thickness. In this program, this was accomplished by measurement of optical interference induced changes in light transmitted through the film. The method was selected because it is the most accurate one available.

Although many techniques have been developed to measure film thickness (e.g., Chopra<sup>1</sup> lists more than 14 methods), only two (optical interference and quartz crystal) are in common usage for monitoring film

---

<sup>1</sup>K.L. Chopra, Thin Film Phenomena, McGraw-Hill (1969).

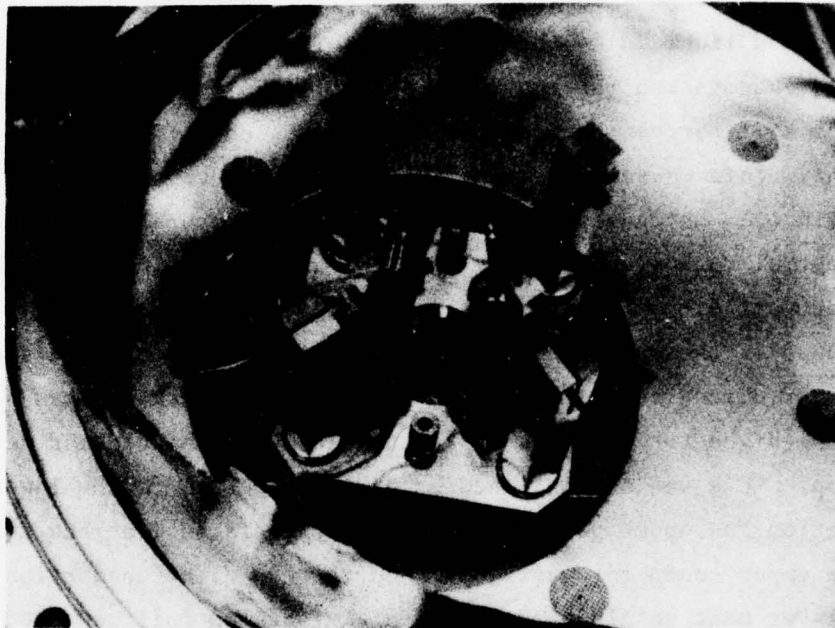


Figure 4. View of the Knudsen type evaporation sources used in this study.

thickness during deposition. The other techniques are restricted as to the materials that can be detected, the sensitivity, the maximum film thickness, the cost of the equipment, or the response time. For these reasons, they have not been used extensively.

The quartz crystal monitor consists of an exposed quartz crystal that is electronically excited. As material is deposited on the crystal, the mass changes and thus the resonant frequency changes. The frequency change is proportional to the mass change (over a limited range) and thus to the film thickness provided the density of the deposited material is constant.

The major problem is that the measurement is not made on the optical substrate so that it is necessary to calibrate the difference in vapor flux to the substrate. The calibration is valid only if the distribution of material from the source remains constant from run to run. In general, this is impossible to achieve because the flux distribution varies as the level of material in the source varies. Another problem is that

the crystal resonance frequency is temperature dependent. As a result, temperature changes in the crystal caused by radiation from the evaporator make it possible to observe "negative" evaporation rates.

The optical method consists of detecting the changes produced by interference effects in the optical film in either the transmission or reflection of the optical monitor beam. The interference-induced maximum or minimum is greatest for the first order and decreases in magnitude with increasing film thickness. Depending on various factors (such as the monitoring wavelength, absorption of the film, scattering in the film, and sensitivity of the electronic circuit), there is a practical upper limit of film thickness that can be accurately measured. In the cases studied in this program, the upper limit was in the range of 2 to 5  $\mu\text{m}$  of film thickness.

The most significant feature is that the thickness determination is made directly on the film that is being deposited. Thus, there is not the calibration problem that exists in the indirect method. Although, in special cases, it is possible to have an accuracy of a few Ångströms in measurement of the film, the accuracy in the present study was in the range of 50 to 100 Å. The choice of monitoring wavelength is of critical importance to the accurate deposition of multilayer AR films. For example, in the deposition of a three-layer AR coating of high, low, and high index of refraction materials on KCl, the first order change in transmission will be a minimum for the high index film and a maximum for the low index film. For best results, it is necessary to correlate the specific optical design and the monitor wavelength so that the first and second layers each terminate exactly on odd orders.

In the laboratory, we have a limited number of narrow band filters, which thus limits the choice of monitoring wavelength. The procedure is to search for a three-layer AR design that has film thicknesses that match to a specific monitor wavelength and produce specific interference patterns. In practice, it generally takes about 10 to 15 different AR designs to obtain a good match to one of the 15 monitor wavelengths.

There is another practical limit in the choice of the monitor wavelength. Although maximum accuracy is obtained by using the shortest wavelength and thus the maximum number of inflection points in the scan, the loss of signal after about 8 fringes restricts the choice. For 9.27  $\mu\text{m}$  AR coatings, the best results were obtained when the monitoring was done in the 1 to 2  $\mu\text{m}$  ranges.

The original apparatus consisted of a broad band light source, a chopper, the sample, a narrow pass band transmission filter, a detector, and the lock-in amplifier circuit shown in Figure 5. We observed that line voltage changes could produce intensity changes in the light source that could be mistaken for the interference effects. As a result, a 3% beam splitter and a detector were added in front of the chopper. This produced a reference signal representing the light source intensity. The detector signal is divided by the reference signal so as to make the output independent of the source variations. The system now has better than 1% stability.

#### D. LASER CALORIMETER

Film absorption is measured using a vacuum calorimeter with a tunable  $\text{CO}_2$  laser. The components are shown in Figure 6. The tunable  $\text{CO}_2$  laser will operate at 9.27, 10.6  $\mu\text{m}$ , and intermediate wavelengths. It has a 1.5 m optical cavity with 1.45 m of active medium. It has a square profile grating with a 6.75  $\mu\text{m}$  period that was ion machined from gold overcoated germanium. The grating does not have a blaze angle and thus has wide angle tunability over the 9 to 11  $\mu\text{m}$  range. The output coupler has a planoconvex configuration with a 4 m radius. It is ZnSe with an 85% reflector coating on the concave surface and a broad band AR coating (centered at 10  $\mu\text{m}$ ) on the plane surface. As the grating is mounted outside the laser tube, the intercavity window also has a broad band AR coating. A 6 mm aperture at the output end limits some of the higher transverse modes. The resulting beam has a reasonably uniform intensity and a circularly shaped cross section.

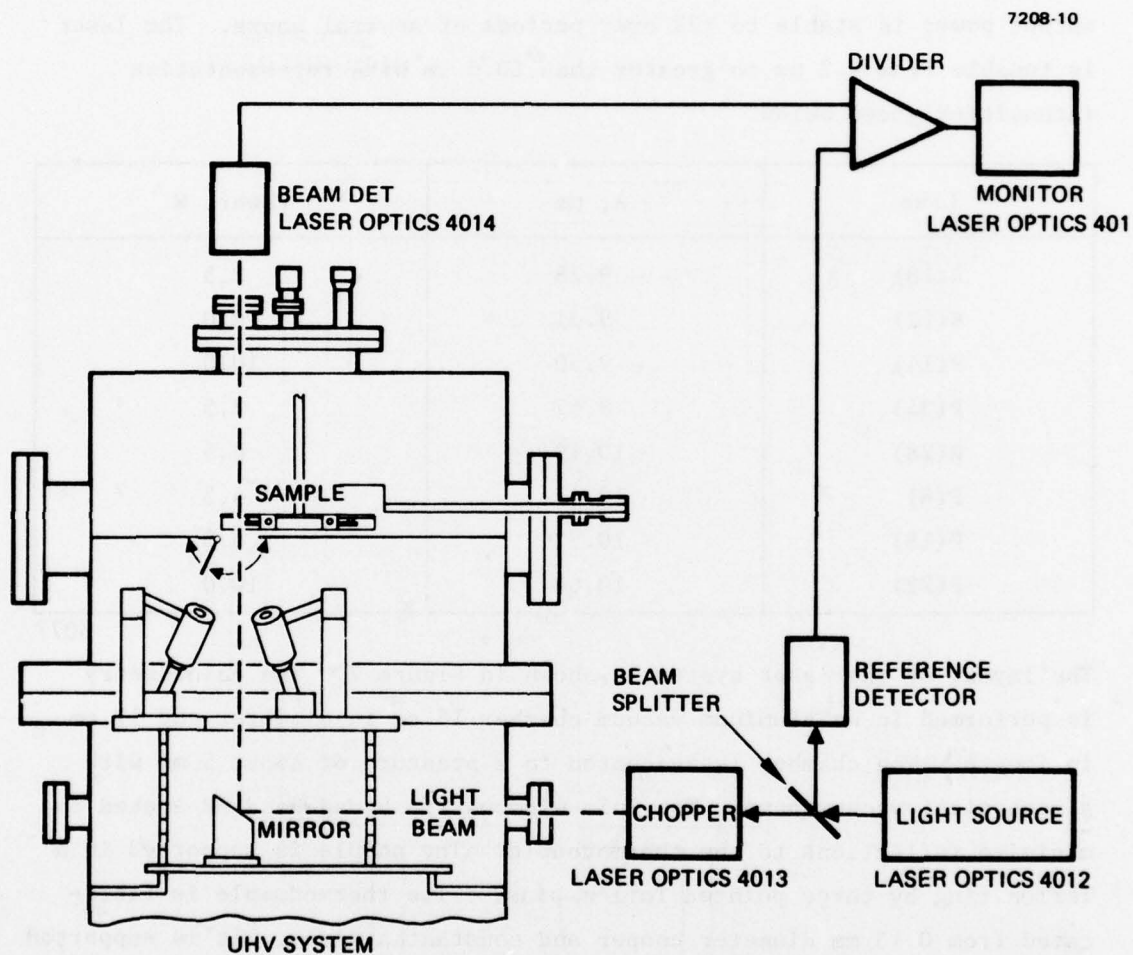


Figure 5. System for the optical monitoring of film thickness during deposition.

The grating is cooled with gaseous  $N_2$  and the laser is water cooled. The laser operated in a flowing mode with a premixed gas consisting of  $CO_2$  (4 to 5%),  $N_2$  (12.5 to 14.5%), and He (the balance). The wavelength stability of the laser using the  $N_2$ -cooled grating is good and the mean output power is stable to  $\pm 2\%$  over periods of several hours. The laser is tunable from 9.2  $\mu m$  to greater than 10.6  $\mu m$  with representative intensities given below.

Line	$\lambda$ , $\mu m$	Power, W
R(18)	9.28	8.5
R(12)	9.31	8.0
P(14)	9.50	10.0
P(34)	9.67	7.5
R(28)	10.19	6.5
P(8)	10.47	4.5
P(18)	10.57	6.8
P(22)	10.60	10.0

6077

The layout of the laser system is shown in Figure 7. The calorimetry is performed in an aluminum vacuum chamber 15 cm in diameter and 17 cm in length. The chamber is evacuated to a pressure of about 5 mm with a mechanical vacuum pump. The ZnSe windows are broad-band AR coated to minimize reflections to the thermocouple. The sample is supported in a Teflon ring by three pointed Teflon pins. The thermocouple is fabricated from 0.13 mm diameter copper and constantan wires. It is supported on a Teflon pin and pressed against the edge of the sample. Dow Corning 346 thermal conductive grease is used to provide good thermal contact. This is shown in Figure 8 and Figure 9.

The samples are mounted in the calorimeter head. After evacuation, the sample is allowed to come to thermal equilibrium. The three slope method (cooling, heating, cooling) is used to determine the absorption. Three separate determinations are made on each sample to minimize the error in determining the heating and cooling slopes.

M12170

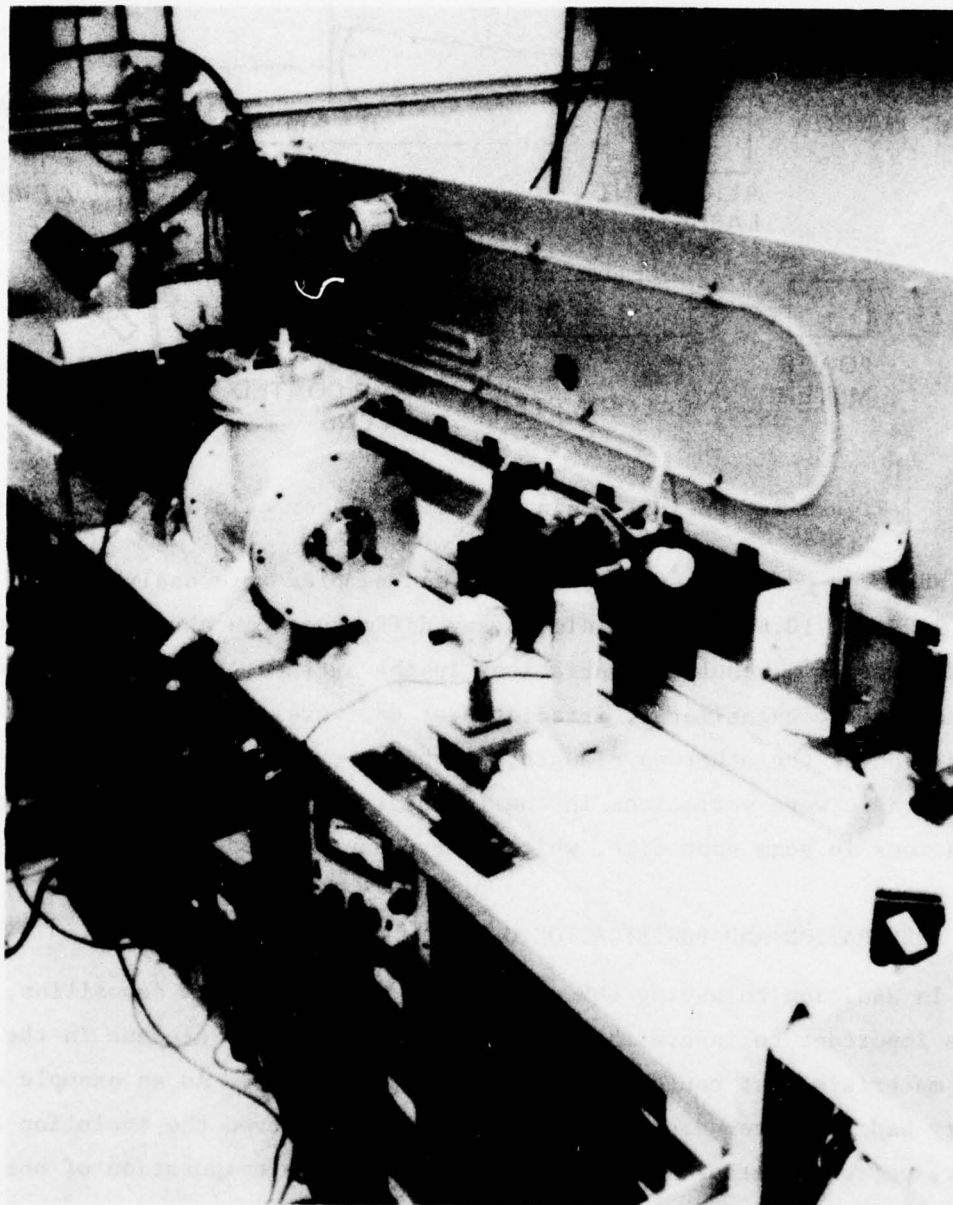


Figure 6. Photograph of laser calorimeter.

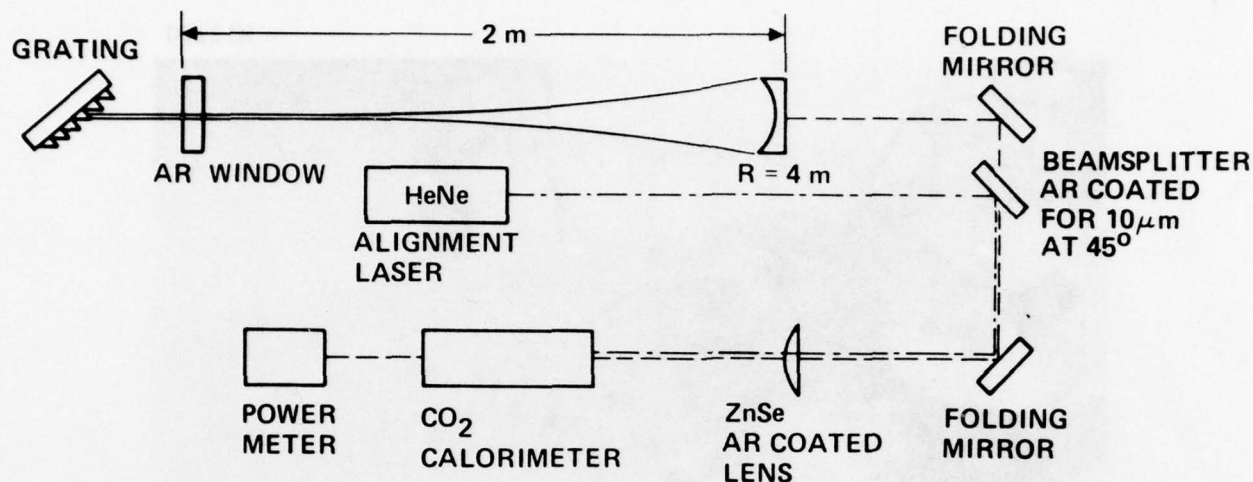


Figure 7. Optical train of the CO<sub>2</sub> laser calorimeter.

Whenever possible, the substrates and samples were analyzed at both 9.27 and 10.6  $\mu\text{m}$ . To minimize any differences in absorption that could occur as a result of variations in the surface, the samples were mounted in the calorimeter, irradiated at one wavelength, and then irradiated at the other wavelength. Although the focal point was constant, there were variations in the irradiated area that resulted from variations in beam spot size, which were caused by mode differences.

#### E. PREPARATION AND PURIFICATION OF FILM MATERIALS

In addition to having UHV conditions during the film deposition, it is important to insure that there are no impurities present in the film materials that could affect the film properties. As an example of a very bad case, seen in another program,<sup>2</sup> we observed the evolution of water, petroleum ether, and acetic acid during the evaporation of one batch of As<sub>2</sub>S<sub>3</sub>. The resulting films had high absorption. As a result, it was necessary to develop methods of preparation of pure materials and of purification of materials which were contaminated.

<sup>2</sup>Laser Window Materials and Optical Coating Science RADC-TR-77-286, August 1977, Interim Technical Report Contract F 19628-76-C-0309.

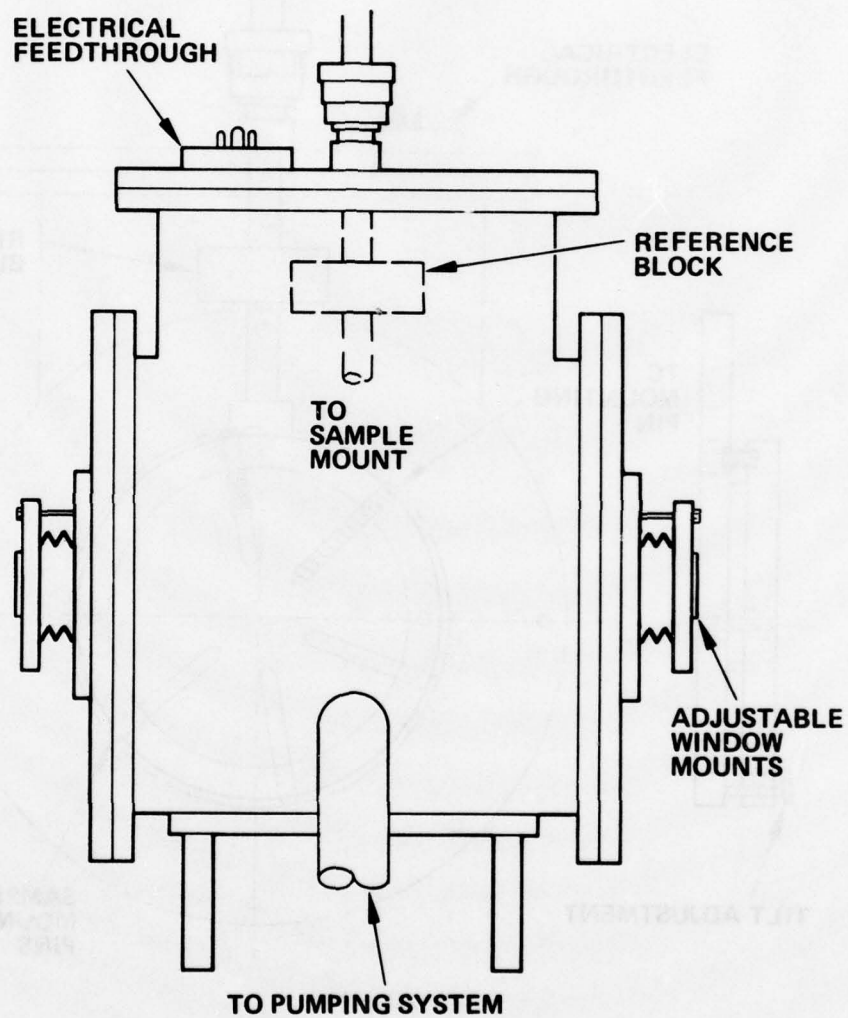


Figure 8. Vacuum calorimeter.

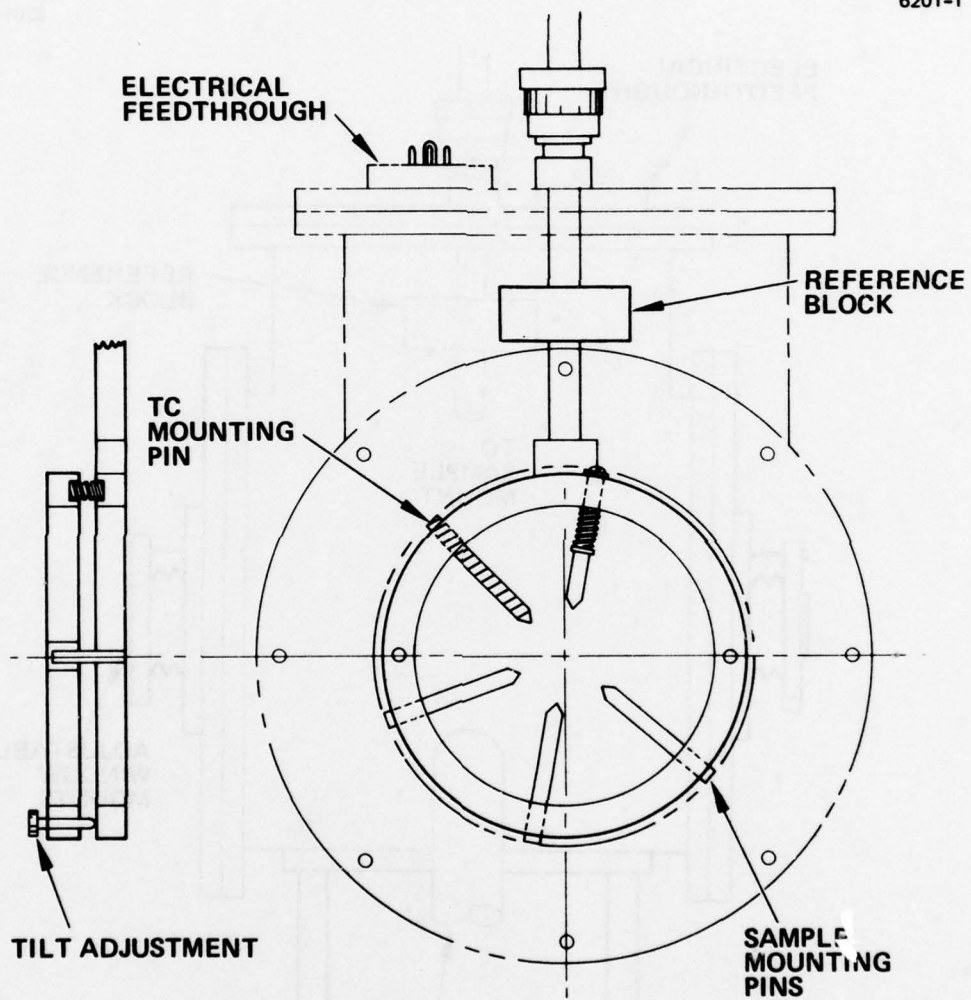


Figure 9. Calorimeter mount for window samples.

Some success was achieved in the preparation of some materials by direct reaction of the elemental forms. For example, in the preparation of either  $\text{As}_2\text{S}_3$  or  $\text{As}_2\text{Se}_3$ , we used a three-chamber silica reactor. The materials were loaded into the end chamber, and then the unit was evacuated under a  $120^\circ\text{C}$  bake-out to remove any absorbed water. The next step was to seal off the system while it is under vacuum. The arsenic is very slowly distilled (in reality, sublimed) into the central chamber. If done carefully, a dark cob-web-like residue is left in the first chamber. This is sealed off and removed. The sulfur or selenium is now distilled into the center chamber and the second chamber is removed. The sealed vial is put in a furnace, allowed to react overnight, and then pulled from the furnace and air quenched.

There are several limitations to the process. It is difficult to obtain sulfur that is water free and arsenic and selenium that are free of oxides. Because of the similarity in vapor pressures, purification by vacuum distillation is not practical. The effect of this can be seen in the transmission spectra of four samples of  $\text{As}_2\text{Se}_3$  which are presented in Figure 10. Samples HRL-1, HRL-2, and HRL-3 were prepared in the manner just described. The HRL-1  $\text{As}_2\text{Se}_3$  was used in all of the  $\text{As}_2\text{Se}_3$  coatings described in this report. The HRL-2 was prepared using 99.999% pure arsenic that had a black surface, which indicated the presence of oxide. The HRL-2 has about 6 strong absorption bands that have been associated with oxide impurities.<sup>3</sup> The same procedure was used to prepare HRL-3. In this case, the arsenic metal used had a metallic (shiny) surface and thus was free of oxide. This is reflected in the transmission spectra.

Because arsenic metal oxidizes immediately on exposure to the atmosphere, it is desirable to transfer the metal from the sealed ampoules to the reaction system under an inert atmosphere or in a vacuum.

---

<sup>3</sup>M. Maklad, et al., "Infrared Transmission in Chalcogenide Glasses," Third Conference on High Power Infrared Laser Window Materials, Nov. 12-14, 1973 AFCRL-TR-74-0085.

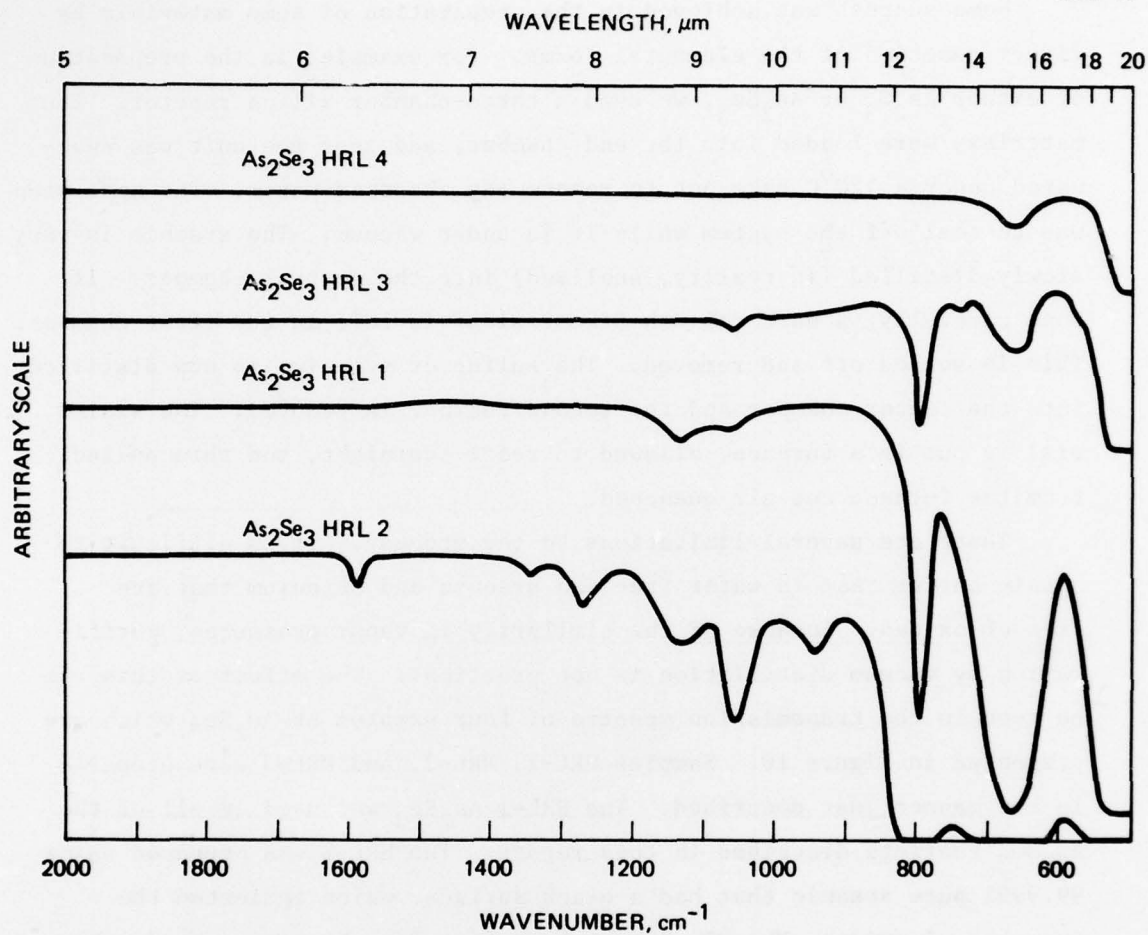


Figure 10. Composite HRL  $\text{As}_2\text{Se}_3$  glasses: HRL-1, HRL-2, HRL-3, and HRL-4.

These facilities were not available, so in the production of HRL-4, the arsenic filled ampoules were cooled to  $\text{LN}_2$  temperature and the transfer made in atmosphere. The low temperature reduced the oxidation of the arsenic to a minimum. This is seen in a comparison of the spectra of HRL-1, HRL-3, and HRL-4.

Purification of contaminated materials is possible if the reaction scheme is carefully selected so as to produce materials which are easily separated from the desired film material.

As an example, take the case where one has material which has the proper stoichiometry but is contaminated with oxides or water. It is possible to remove these by means of a chemical reaction. In the case of  $\text{As}_2\text{Se}_3$ , this would involve passing the  $\text{As}_2\text{Se}_3$  vapor through graphite heated to 800 to 900°C.

#### F. LASER DAMAGE THRESHOLD TESTS

Samples of three layer AR coatings and of single layer coatings were submitted for laser damage threshold tests under the direction of J. A. Detrio. Although the tests were not a direct part of this effort, the results are of interest in presenting a complete discussion of these coatings. As a consequence, the apparatus is described briefly here and the results are presented in Section III.

The focused laser damage measurements were performed using the apparatus described by J. A. Detrio.<sup>4</sup> The broad beam high power testing (with spot size of about  $1 \text{ cm}^2$ ) was done at 10.6 and 9.28  $\mu\text{m}$  with an Electro Aerodynamic Laser operating in a master-oscillator - power-amplifier configuration. The wavelength was varied by the use of a grating mounted in the Coherent Radiation Laboratories Model 41 laser oscillator. The samples were mounted just ahead of the focus of a 2 m radius mirror. The beam profile was not Gaussian, but every effort was made to maintain a constant beam profile between the two wavelengths. The power was measured with a total capture ballistic calorimeter and each irradiation was monitored with a fast response detector.

The power density reported for the broad beam damage thresholds is an average value obtained by attempting to weigh the power distribution by the area covered. When the EAL was driven to operate nominally at 9.28  $\mu\text{m}$ , the laser emission occurs predominantly from the R18 transition centered at near 9.28  $\mu\text{m}$ . Other lines at 9.26 and 9.27  $\mu\text{m}$  are also observed. The beam profile was obtained by examining burn patterns in

---

<sup>4</sup>J. A. Detrio, R. D. Petty, M. C. Ohmer, and O. F. Swenson, "Laser Induced Damage in Optical Materials," 1976, NBS Special Publication 462, pg. 283.

plexiglass. The burn patterns were made as a function of power and the full width at half maximum depth was measured on an optical comparator.

The beam profile can best be described as a central peak surrounded by a region of amplified edge diffraction. Every reasonable attempt was made to ensure that the beam profile was the same at 10.6 and 9.28  $\mu\text{m}$ . In spite of these efforts, the beam profiles, although superficially identical, were different at the two wavelengths, especially within the central hot spot. The average power density over the entire beam (central peak and surrounding area) is nearly equal with a total area of 1.5  $\text{cm}^2$ . The central hot spot was 0.17  $\text{cm}$  at 10.6  $\mu\text{m}$  and 0.06  $\text{cm}^2$  at 9.28  $\mu\text{m}$ .

The focused beam tests were performed at 10.6  $\mu\text{m}$  with a Gaussian beam profile of 0.1  $\text{cm}$  diameter. Both n-on-1 and 1-on-1 tests were made on a 4 by 4 array of test points spaced 3 mm apart. Some 3.5-cm-diameter samples were tested with a 9 point test array.

### SECTION III

#### DISCUSSION OF RESULTS

AR coatings of ZnSe/KCl/ZnSe,  $\text{As}_2\text{S}_3/\text{KCl}/\text{As}_2\text{S}_3$ ,  $\text{As}_2\text{Se}_3/\text{KCl}/\text{As}_2\text{Se}_3$ ,  $\text{As}_2\text{Se}_3/\text{NaF}/\text{As}_2\text{Se}_3$ , and TlI/KCl/TlI were designed, developed, and analyzed in this program in that chronological order. Although the major effort was directed to the TlI coatings, we present the results in chronological order.

#### A. ZnSe/KCl/ZnSe COATING RESULTS

The ZnSe/KCl/ZnSe system was selected to be the first AR coating investigated in this program. Although it is not an ideal coating for KCl because of its sensitivity to stress cracking, 10.6  $\mu\text{m}$  AR designs had been studied in detail in a previous program<sup>5</sup> and thus this system is well understood. For this reason, it was decided to deposit 9.27  $\mu\text{m}$  AR coatings of ZnSe/KCl/ZnSe to verify the operation of the new deposition system.

Three AR coating designs were developed. These are listed in Table 1. In three runs, a total of 12 samples were deposited. The results are presented in Table 2.

Table 1. ZnSe/KCl/ZnSe AR Coating Designs

Design	Film Thickness, $\mu\text{m}$			Theoretical Absorption, % per Surface
	ZnSe	KCl	ZnSe	
Z1	1.145	0.406	0.425	0.016
Z2	1.129	0.412	0.430	0.016
Z3	0.617	0.891	0.359	0.013

6077

<sup>5</sup>Laser Window Surface Finishing and Coating Science RADC-77-40 Final Technical Report, January 1977, Contract No. F 19628-75-C-0135.

Table 2. Summary of ZnSe/KCl/ZnSe AR Coating Results

Sample No.	Substrate Dopant	Coating Design	Transmission Peak, $\mu\text{m}$	9.27 $\mu\text{m}$ Absorption			Remarks
				Substrate, %	Sample, %	Coating, % per Surface	
1272-2-1	Eu	Z3	9.56	0.114	0.568	0.23	Open $\text{As}_2\text{S}_3$ and $\text{As}_2\text{Se}_3$ sources
1277-2-2	Eu	Z3	9.24	0.172	0.235	0.031	
1274-2-3	Eu	Z2	9.35	0.085	0.390	0.15	
1273-2-4	Eu	Z1	9.40	0.068	0.652	0.29	
1281-3-1	Eu	Z1	9.56	0.156	0.242	0.043	Covered $\text{As}_2\text{S}_3$ and $\text{As}_2\text{Se}_3$ sources
1280-3-2	Eu	Z1	9.51	0.085	0.292	0.10	
9-2-3-3	Rb	Z1	9.43	0.187	0.444	0.13	
9-3-3-4	Rb	Z1	9.46	0.134	0.486	0.18	
9-5-4-1	Rb	Z1	9.39	0.133	0.394	0.13	Covered $\text{As}_2\text{S}_3$ and $\text{As}_2\text{Se}_3$ sources small leak in Cu wire seal resulted in $\text{H}_2\text{O}$ partial pressure of 2 x 10 <sup>-9</sup> Torr
9-15-4-2	Rb	Z1	9.30	0.20	0.440	0.12	
1282-4-3	Eu	Z1	9.24	0.097	0.225	0.064	
1288-4-4	Eu	Z1	9.16	0.093	0.266	0.086	

5077

Transmission spectra of three of the four samples produced in the first run exhibited a pronounced (2 to 3%) absorption at 9.0  $\mu\text{m}$ . A typical case, the transmission spectrum of sample 1272-2-1, is shown in Figure 11. In sample 12-7-2-2, No. 9.0  $\mu\text{m}$  absorption was observed.

Similar 9.0  $\mu\text{m}$  absorption dips were observed in other programs on studies of films containing either  $\text{As}_2\text{S}_3$  or  $\text{As}_2\text{Se}_3$ . After an analysis, it was determined that the source of the absorption was an arsenic oxide impurity in the films.

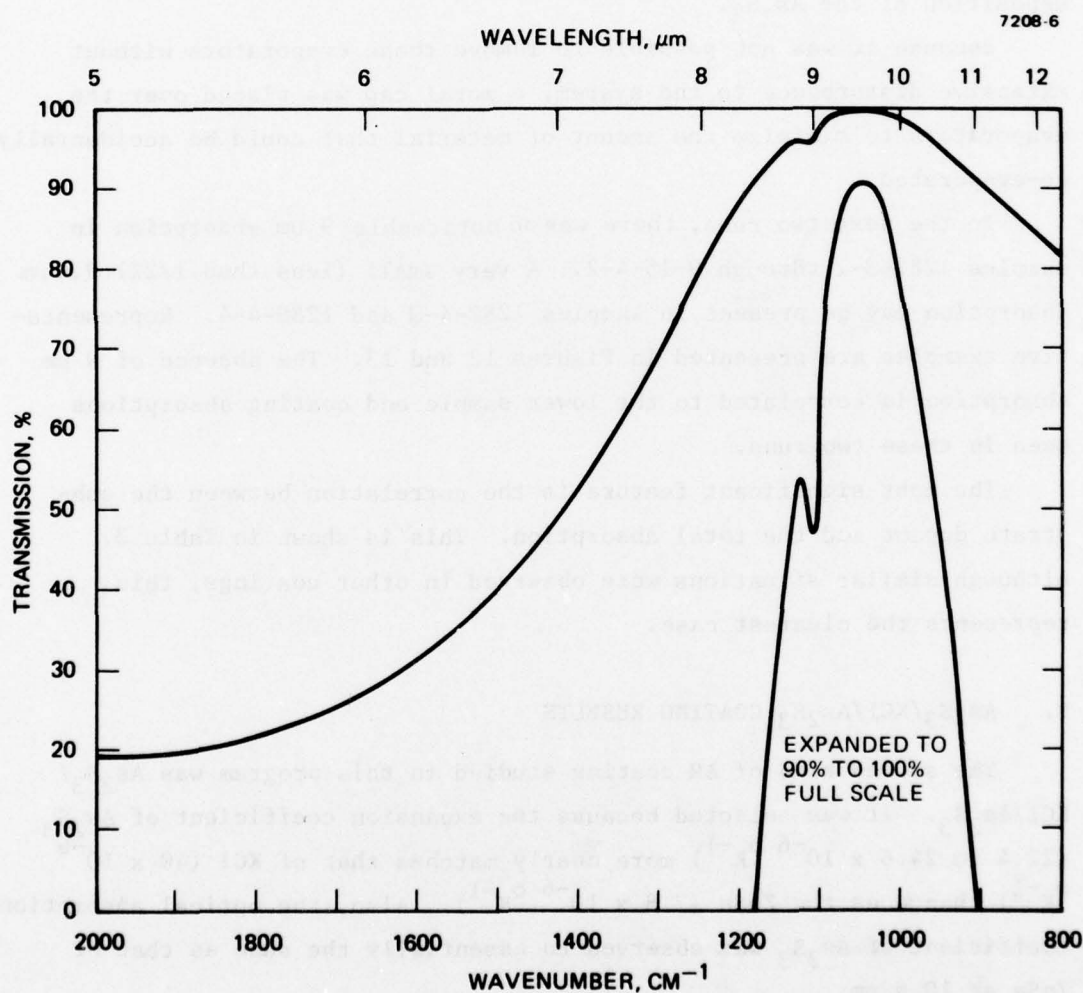


Figure 11. Transmission spectra of 1272-2-1 (ZnSe/KCl/ZnSe AR coating), which exhibits oxide related absorption at 9  $\mu\text{m}$ .

In the present case, the evaporation system contained six close-spaced evaporation sources. These had been loaded with  $\text{ThF}_4$ ,  $\text{KCl}$ ,  $\text{NaF}$ ,  $\text{ZnSe}$ ,  $\text{As}_2\text{S}_3$ , and  $\text{As}_2\text{Se}_3$  before the first run. It is believed that the evaporation of  $\text{ZnSe}$  at  $1100^\circ\text{C}$  caused the warming of the adjacent cell, which contained  $\text{As}_2\text{S}_3$ , manufactured by the Atomergic Chemical Corporation. This same material had been analyzed by mass spectrometry in another program (Contract F19628-76-C-0309) and found to evolve significant amounts of water vapor, petroleum ether, and acetic acid during the deposition of the  $\text{As}_2\text{S}_3$ .

Because it was not possible to remove these evaporators without extensive disturbance to the system, a metal cap was placed over the evaporators to minimize the amount of material that could be accidentally co-evaporated.

In the next two runs, there was no noticeable  $9\text{ }\mu\text{m}$  absorption in samples 1281-3-1 through 9-15-4-2. A very small (less than 1/2%)  $9.0\text{ }\mu\text{m}$  absorption may be present in samples 1282-4-3 and 1288-4-4. Representative examples are presented in Figures 12 and 13. The absence of  $9\text{ }\mu\text{m}$  absorption is correlated to the lower sample and coating absorptions seen in these two runs.

The most significant feature is the correlation between the substrate dopant and the total absorption. This is shown in Table 3. Although similar situations were observed in other coatings, this represents the clearest case.

#### B. $\text{As}_2\text{S}_3/\text{KCl}/\text{As}_2\text{S}_3$ COATING RESULTS

The second kind of AR coating studied in this program was  $\text{As}_2\text{S}_3/\text{KCl}/\text{As}_2\text{S}_3$ . It was selected because the expansion coefficient of  $\text{As}_2\text{S}_3$  ( $22.4$  to  $24.6 \times 10^{-6} \text{ }^\circ\text{K}^{-1}$ ) more nearly matches that of  $\text{KCl}$  ( $40 \times 10^{-6} \text{ }^\circ\text{K}^{-1}$ ) than does the  $\text{ZnSe}$  ( $7.8 \times 10^{-6} \text{ }^\circ\text{K}^{-1}$ ). Also, the optical absorption coefficient of  $\text{As}_2\text{S}_3$  was observed to essentially the same as that of  $\text{ZnSe}$  at  $10.6\text{ }\mu\text{m}$ .

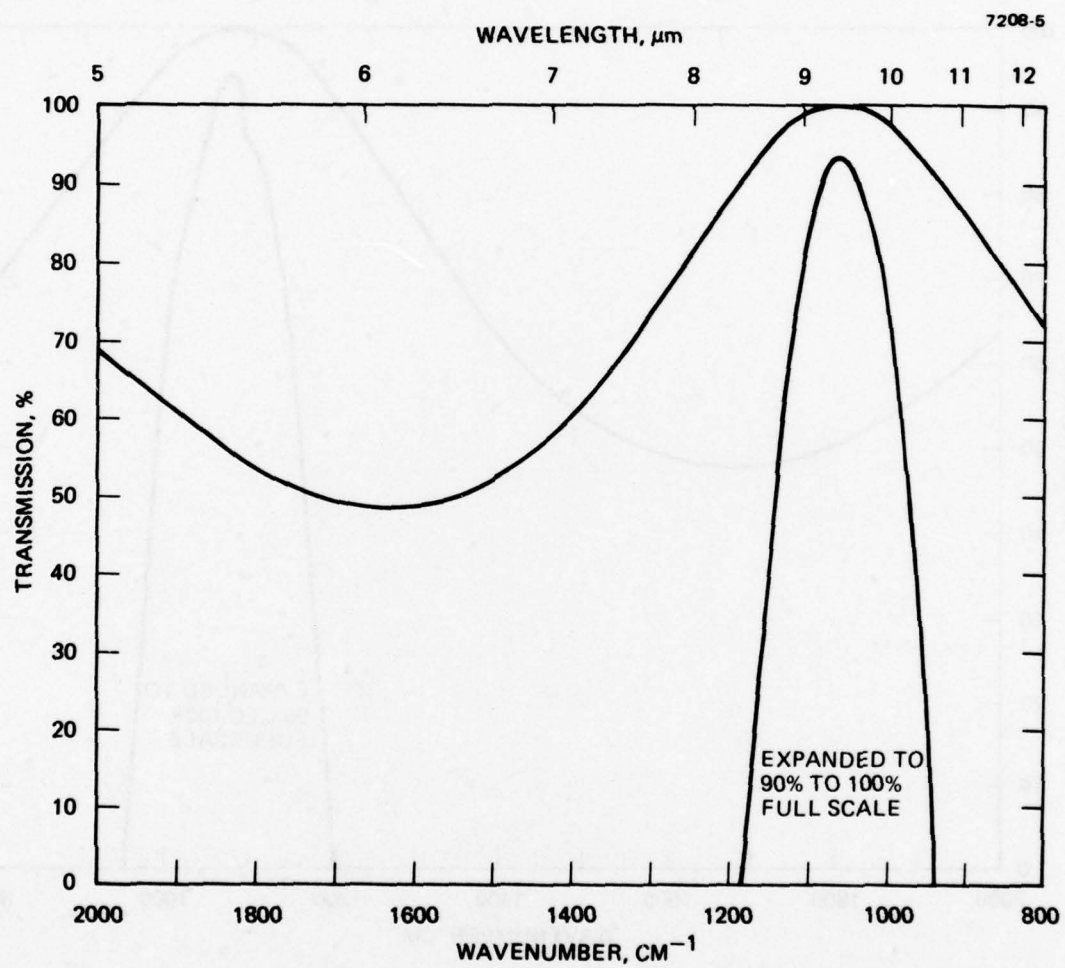


Figure 12. Transmission spectra of 9-2-3-3 (ZnSe/KCl/ZnSe AR coating).

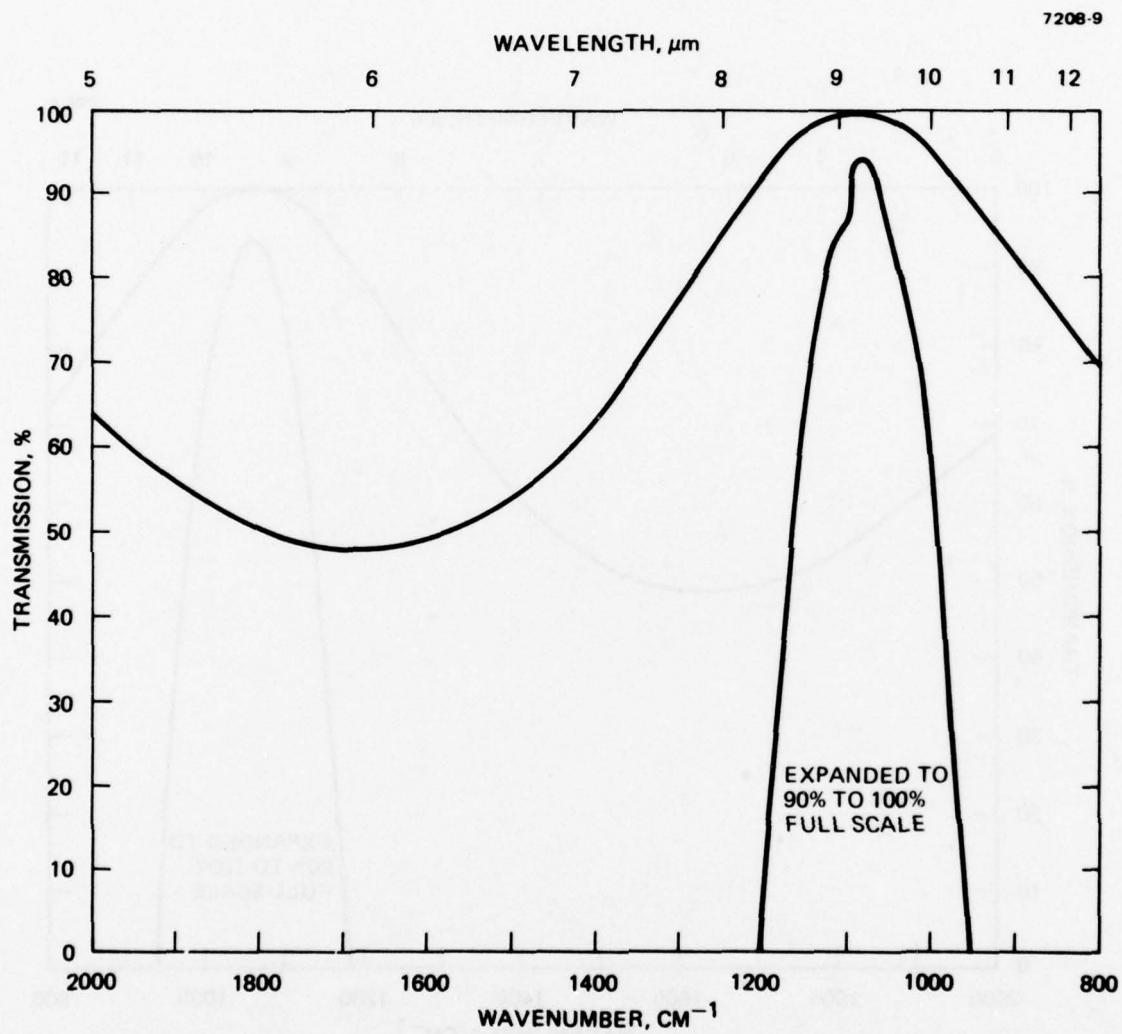


Figure 13. Transmission spectra of 1282-4-3 (ZnSe/KCl/ZnSe AR coating).

Table 3. Comparison of Sample Absorption with Substrate Dopant

Sample Type	Total Absorption, $\text{cm}^{-1}$	Sample Absorption, %	Coating Absorption, % per Surface
Europium doped KCl			
1281-3-1	0.00239	0.242	0.043
1280-3-2	0.00289	0.292	0.10
1282-4-3	0.00233	0.225	0.064
1288-4-4	0.00274	0.266	0.086
Rubidium doped KCl			
9-2-3-3	0.00446	0.444	0.13
9-3-3-4	0.00484	0.486	0.18
9-5-4-1	0.00382	0.394	0.13
9-15-4-2	0.00439	0.440	0.12

6077

Difficulties in controlling the deposition rate of  $\text{As}_2\text{S}_3$  resulted from the use of the old style evaporator which had the hottest region at the center of the evaporator. The molten  $\text{As}_2\text{S}_3$  forms a viscous liquid. As we tried to attain a useful deposition rate, gas bubbles would form. These would either burst through the surface or expel a plug of  $\text{As}_2\text{S}_3$  to the top of the evaporator. Both conditions produced a sudden and very rapid change in the deposition rate.

Because of these problems, only a single run was made. The results of single layer films and AR films are shown in Table 4. The transmission spectrum of sample 9-12-5-4 is shown in Figure 14.

#### C. $\text{As}_2\text{Se}_3/\text{KCl}/\text{As}_2\text{Se}_3$ RESULTS

The third system studied was that of  $\text{As}_2\text{Se}_3/\text{KCl}/\text{As}_2\text{Se}_3$ . The expansion coefficient and absorption coefficient of  $\text{As}_2\text{Se}_3$  have essentially the same values as  $\text{As}_2\text{S}_3$ . While the evaporation of  $\text{As}_2\text{Se}_3$  is much less sensitive to the problem of pressure bursts (as was observed in the  $\text{As}_2\text{S}_3$  case), the  $\text{As}_2\text{Se}_3$  is more sensitive to oxidation than is the  $\text{As}_2\text{S}_3$ .

Table 4.  $\text{As}_2\text{S}_3/\text{KCl}/\text{As}_2\text{S}_3$  Data

Sample Number <sup>a</sup>	Coating Design	Transmission Peak, $\mu\text{m}$	Absorption Data								Remarks
			9.27 $\mu\text{m}$				10.6 $\mu\text{m}$				
			Substrate, %	Sample, %	Coating, % per Surface	Absorption Coefficient, $\text{cm}^{-1}$	Substrate, %	Sample, %	Coating, % per Surface	Absorption Coefficient, $\text{cm}^{-1}$	
9-12-5-4	AR	9.0	0.040	0.177	0.069		b	b			0.488 $\mu\text{m}$ $\text{As}_2\text{S}_3/1.144 \mu\text{m}$ $\text{KCl}/0.279 \mu\text{m}$ $\text{As}_2\text{S}_3$
4-16-5-1	1.5 $\lambda$	9.2	0.240	0.361	0.12	1.4	b	0.144	<0.14	<3.2	5.87 $\mu\text{m}$ $\text{As}_2\text{S}_3$
8-4-5-2	0.5 $\lambda$	9.75	0.188	0.325	0.14	6.2	b	b			2.06 $\mu\text{m}$ $\text{As}_2\text{S}_3$
9-1-5-3	0.5 $\lambda$	9.75	0.081	0.270	0.19	8.4	b	b			2.06 $\mu\text{m}$ $\text{As}_2\text{S}_3$

<sup>a</sup>All samples RB doped.

<sup>b</sup>Not measured.

6077

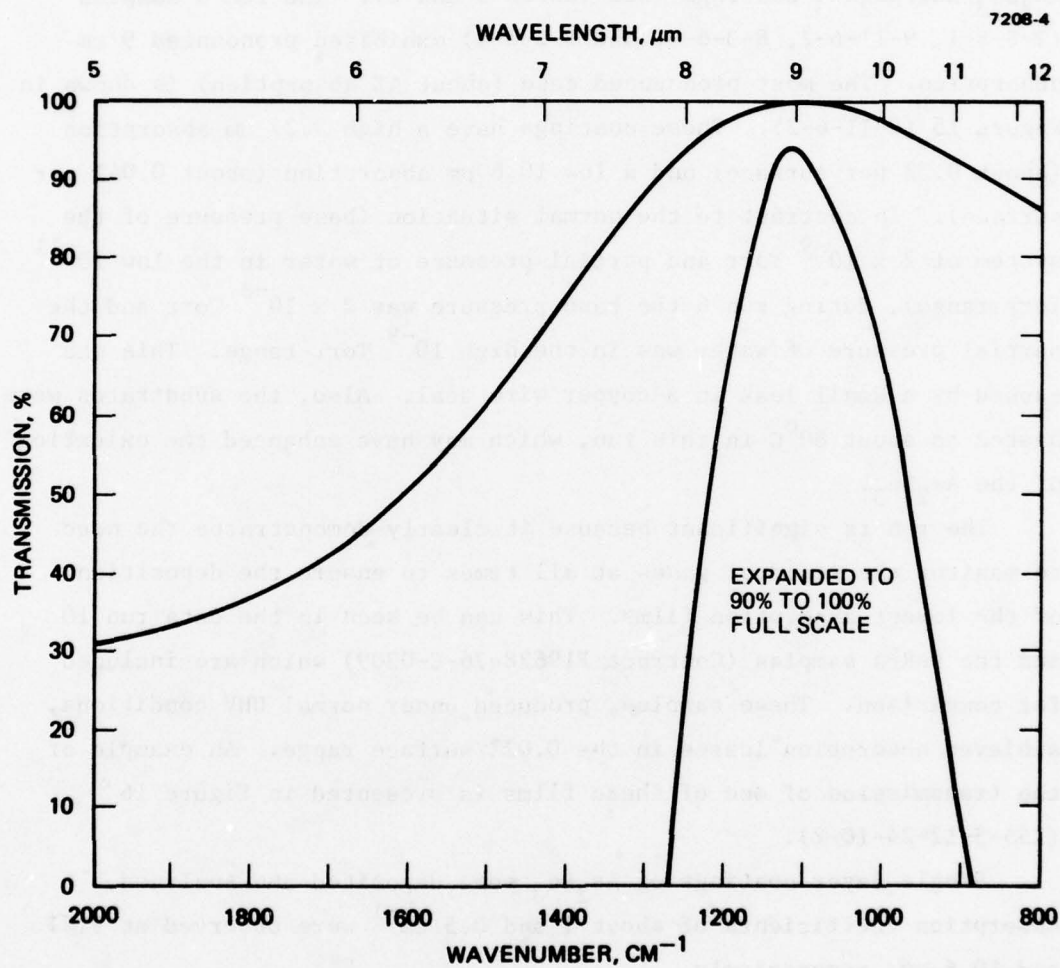


Figure 14. Transmission spectra of 9-12-5-4  
( $\text{As}_2\text{S}_3/\text{KCl}/\text{As}_2\text{S}_3$  AR coating)

The presence of oxide in the coating is manifest as a strong  $9.0\text{ }\mu\text{m}$  absorption. Vaško reports that of the three forms of the arsenic oxide (cubic, monoclinic, and glassy), the glassy state is similar to the monoclinic and both have a strong  $9\text{ }\mu\text{m}$  absorption band.<sup>6</sup>

An example of this behavior was observed in the first set of  $\text{As}_2\text{Se}_3/\text{KCl}/\text{As}_2\text{Se}_3$  coatings (see Tables 5 and 6). The run 6 samples (9-8-6-1, 9-11-6-2, 8-3-6-3, and 8-2-6-4) exhibited pronounced  $9\text{ }\mu\text{m}$  absorption. The most pronounced case (about 4% absorption) is shown in Figure 15 (9-11-6-2). These coatings have a high  $9.27\text{ }\mu\text{m}$  absorption (about 0.3% per surface) and a low  $10.6\text{ }\mu\text{m}$  absorption (about 0.04% per surface). In contrast to the normal situation (base pressure of the system of  $2 \times 10^{-9}$  Torr and partial pressure of water in the low  $10^{-11}$  Torr range), during run 6 the base pressure was  $2 \times 10^{-8}$  Torr and the partial pressure of water was in the high  $10^{-9}$  Torr range. This was caused by a small leak in a copper wire seal. Also, the substrates were heated to about  $80^\circ\text{C}$  in this run, which may have enhanced the oxidation of the  $\text{As}_2\text{Se}_3$ .

The run is significant because it clearly demonstrates the need to monitor the residual gases at all times to ensure the deposition of the lowest absorption films. This can be seen in the data run 10 and the DARPA samples (Contract F19628-76-C-0309) which are included for comparison. These samples, produced under normal UHV conditions, achieved absorption losses in the 0.02%/surface range. An example of the transmission of one of these films is presented in Figure 16 (155-5-12-24-10-2).

Single layer coatings of  $\text{As}_2\text{Se}_3$  were deposited and analyzed. Absorption coefficients of about 1 and  $0.5\text{ cm}^{-1}$  were observed at  $9.27$  and  $10.6\text{ }\mu\text{m}$ , respectively.

---

<sup>6</sup> A. Vaško, D. Ležal, and I. Srb, Journal of Non-Crystalline Solids, 4, 311-21 (1970).

Table 5. Summary of  $\text{As}_2\text{Se}_3/\text{KCl}/\text{As}_2\text{Se}_3$  AR and  $\text{As}_2\text{Se}_3$  Single Layer Coating Data

Sample No.	Substrate Dopant	Coating Design	Transmission Peak, m	Absorption Data								Remarks
				9.27 $\mu\text{m}$				10.6 $\mu\text{m}$				
				Substrate, %	Sample, %	Coating, % per Surface	Absorption Coefficient, $\text{cm}^{-1}$	Substrate, %	Sample, %	Coating, % per Surface	Absorption Coefficient, $\text{cm}^{-1}$	
9-8-6-1	Rb	E1	10.44	0.064	0.77	0.35		(a)	0.108	<0.054		Run 6 small leaks in Cu wire seal - base pressing $P = 2 \times 10^{-8}$ ( $\text{H}_2\text{O}$ major gas present)
9-11-6-2	Rb	E2	9.34	0.081	0.72	0.32		(a)	0.080	<0.040		
8-3-6-3	Rb	E2	9.83	0.13	0.85	0.36		0.039	0.135	0.048		
8-2-6-4	Rb	E2	9.94	0.063	0.73	0.33		0.035	0.103	0.034		
174-6-35-10-1	Rb	E2	8.42	(a)	0.50	<0.25		(a)	1.03	<0.51		
155-5-12-10-2	Rb	E3	10.55	0.080	0.26	0.090		0.065	0.099	0.017		
BF64-25-10-3	Undoped	E4	10.50	0.053	0.26	0.105		0.021	0.087	0.033		
BF64-26-10-4	Undoped	E5	10.50	0.050	0.29	0.12		0.022	0.104	0.041		
150-4-15-7-3	Rb	1 $\lambda$	9.45	0.092	0.226	0.13	3.25	0.097	0.113	0.016	0.53	
155-5-13-8-4	Rb	1 $\lambda$	9.62	0.075	0.164	0.090	2.30	0.073	0.052	<0.052	<1.60	
174-8-31-9-3	Rb	1/2 $\lambda$	9.62	0.107	0.219	0.056	2.72	0.023	0.060	0.019	1.08	
174-5-29-9-4	Rb	1 $\lambda$	9.44	0.045	0.099	0.045	1.13	0.028	0.056	0.028	0.99	
164-5A-10-48-3	Rb	E1	9.36	0.137	0.211	0.037		(a)	0.059	<0.030		DARPA sample
164-5A-11-48-4	Rb	E1	9.67	0.111	0.148	0.019		(a)	0.045	<0.022		DARPA sample
129-1-49-1	Single crystal	E1	9.2	0.098	0.094	<0.047		0.026	0.079	0.026		DARPA sample
129-2-49-2	Single crystal	E1	9.8	0.071	0.148	0.039		0.021	0.156	0.068		DARPA sample

<sup>a</sup>not measured.

<sup>a</sup> not measured.

Table 6.  $\text{As}_2\text{Se}_3/\text{KCl}/\text{As}_2\text{Se}_3$   
AR Coating Designs

Design	Film Thickness, $\mu\text{m}$		
	$\text{As}_3\text{Se}_3$	KCl	$\text{As}_2\text{Se}_3$
E1	0.556	0.742	0.352
E2	0.729	0.492	0.421
E3	0.881	0.504	0.488
E4	0.982	0.422	0.490
E5	1.007	0.406	0.487

6077

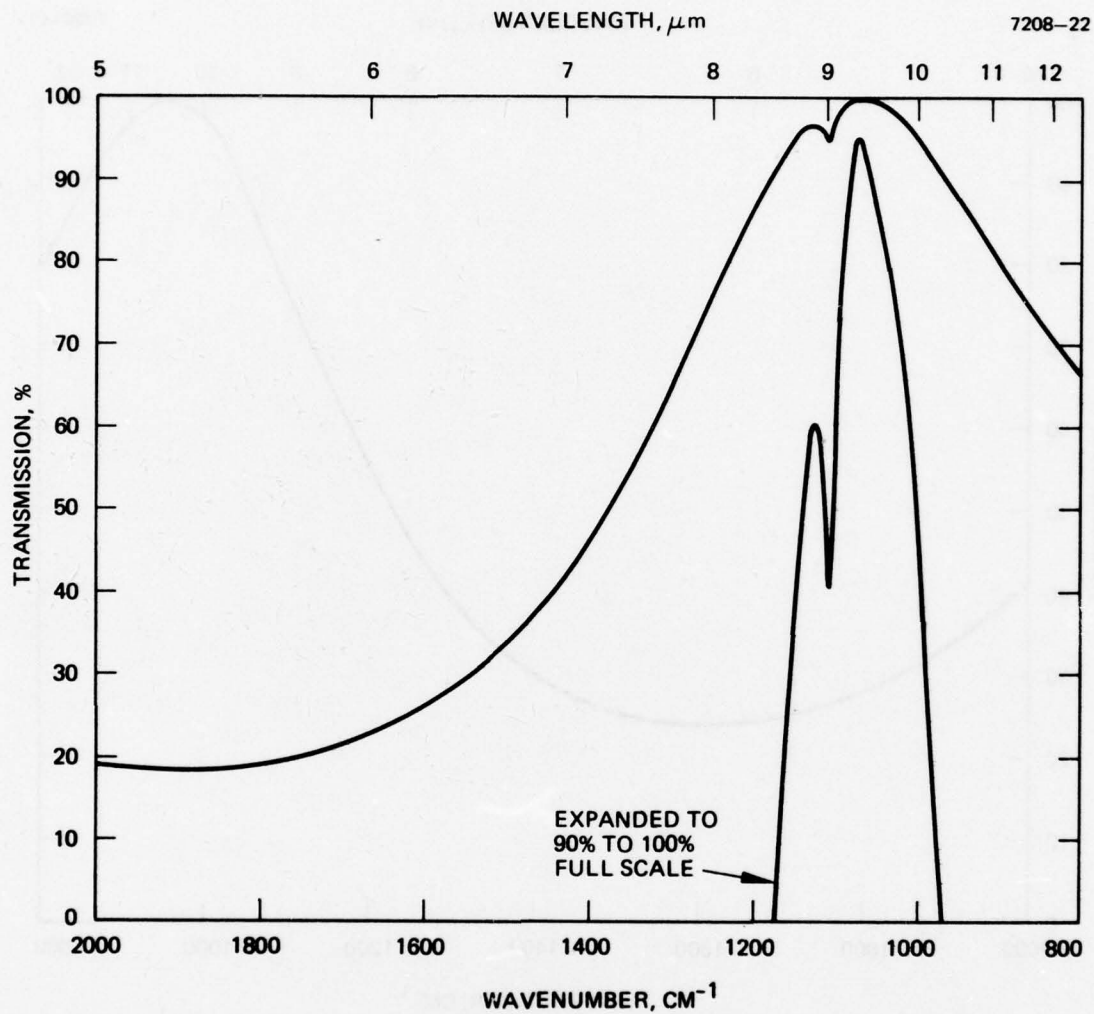


Figure 15. Transmission spectra of 9-11-6-2 ( $\text{As}_2\text{Se}_3/\text{KCl}/\text{As}_2\text{Se}_3$  AR coating), which exhibits strong 9  $\mu\text{m}$  absorption.

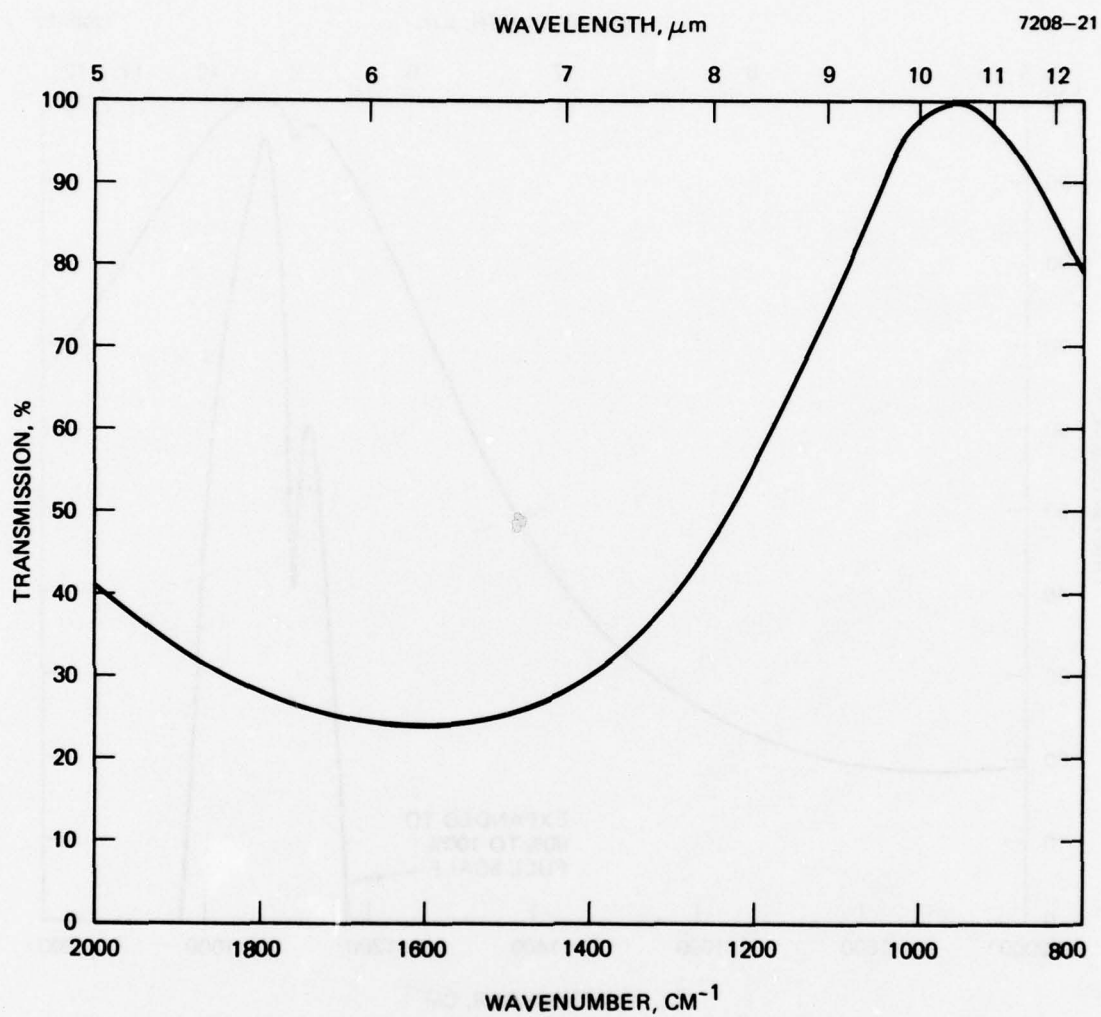


Figure 16. Transmission spectra of 155-5-12-24-10-2 ( $\text{As}_2\text{Se}_3/\text{KCl}/\text{As}_2\text{Se}_3$  AR coating).

#### D. $\text{As}_2\text{Se}_3/\text{NaF}/\text{As}_2\text{Se}_3$ RESULTS

In addition to having low optical absorption and reflection losses, a good AR coating must resist the effects of humidity. Because the solubility of NaF is about 10% of the KCl value, it was used in the  $\text{As}_2\text{Se}_3/\text{NaF}/\text{As}_2\text{Se}_3$  AR coating study. A broadband AR coating centered at  $9.27\text{ }\mu\text{m}$  was designed. The film thicknesses for run 7 samples were  $0.418\text{ }\mu\text{m}$  of  $\text{As}_2\text{Se}_3$ ,  $0.927\text{ }\mu\text{m}$  of NaF, and  $0.297\text{ }\mu\text{m}$  of  $\text{As}_2\text{Se}_3$  as the last (outside) layer.

In the first attempt, we found that the NaF had reacted with the  $\text{SiO}_2$  liner that is used in the evaporator. This resulted in a very high film absorption (0.6 to 1.3% per surface rather than the theoretical value of 0.08% per surface), which is shown in Table 7. The high absorption is believed to be due to the incorporation of  $\text{SiF}_4$  into the film. The  $\text{SiF}_4$ , which results from the reaction of NaF and  $\text{SiO}_2$ , was identified by means of a mass spectrometer analysis. In addition, the transmission scan of sample 9-10-7-1 and the scan of 150-4-14-7-4 show a significant absorption at  $13.6\text{ }\mu\text{m}$ . These are seen in Figures 17 and 18.

We tried to prevent this reaction by depositing a layer of pyrolytic carbon on the interior surface of the  $\text{SiO}_2$  liner. Although the reaction with NaF was reduced considerably, the carbon was evaporated onto the sample and caused a very high absorption. It is believed that the NaF attacked the liner through pin holes in the pyrolytic carbon layer.

A palladium liner was fabricated and used to contain the NaF. Two coatings were deposited successfully in run 9. A new  $\text{As}_2\text{Se}_3/\text{NaF}/\text{As}_2\text{Se}_3$  coating design ( $0.641\text{ }\mu\text{m}$   $\text{As}_2\text{Se}_3$ ,  $0.557\text{ }\mu\text{m}$  NaF,  $0.414\text{ }\mu\text{m}$   $\text{As}_2\text{Se}_3$ ) was used. Sample 174-5-30-9-1 (see Figure 19) had a  $9.27\text{ }\mu\text{m}$  absorption of 0.033% per surface and a transmission peak at  $9.30\text{ }\mu\text{m}$ . The second sample (174-8-33-9-2) had one of the NaF layers overrun to  $0.86\text{ }\mu\text{m}$ . As a result, the transmission peak shifted to  $10.0\text{ }\mu\text{m}$ . In sharp contrast to the previous cases, this coating had a lower  $9.27\text{ }\mu\text{m}$  absorption than its  $10.6\text{ }\mu\text{m}$  value. This is possibly due to the presence of the long wave cut-off in NaF.

Table 7.  $\text{As}_2\text{Se}_3/\text{NaF}/\text{As}_2\text{Se}_3$  Data

Sample No.	Substrate Dopant	Transmission, Peak, $\mu\text{m}$	Absorption Data					
			9.27 $\mu\text{m}$			10.6 $\mu\text{m}$		
			Substrate, %	Sample, %	Coating, % per Surface	Substrate, %	Sample, %	Coating, % per Surface
9-10-7-1	Rb	8.90	0.145	1.277	0.57	0.109	1.094	0.49
150-4-14-7-4	Rb	9.35	0.070	2.716	1.32	0.058	1.773	0.86
174-5-30-9-1	Rb	9.30	0.167	0.233	0.033	0.055	0.382	0.16
174-8-33-9-2	Rb	10.0	0.079	0.237	0.079	0.142	0.678	0.27

6077

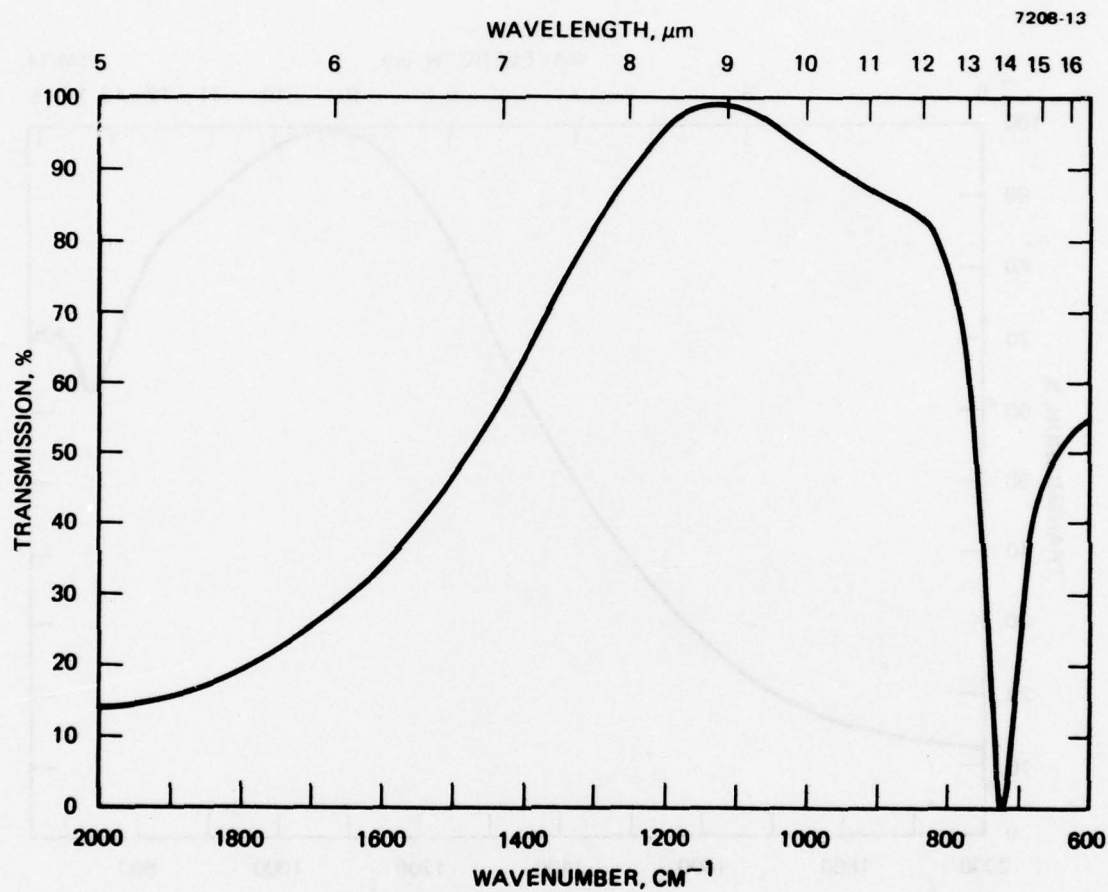


Figure 17. Transmission spectra of 9-10-7-1 (As<sub>2</sub>Se<sub>3</sub>/NaF/As<sub>2</sub>Se<sub>3</sub> AR coating), which exhibits strong 13.6 μm absorption.

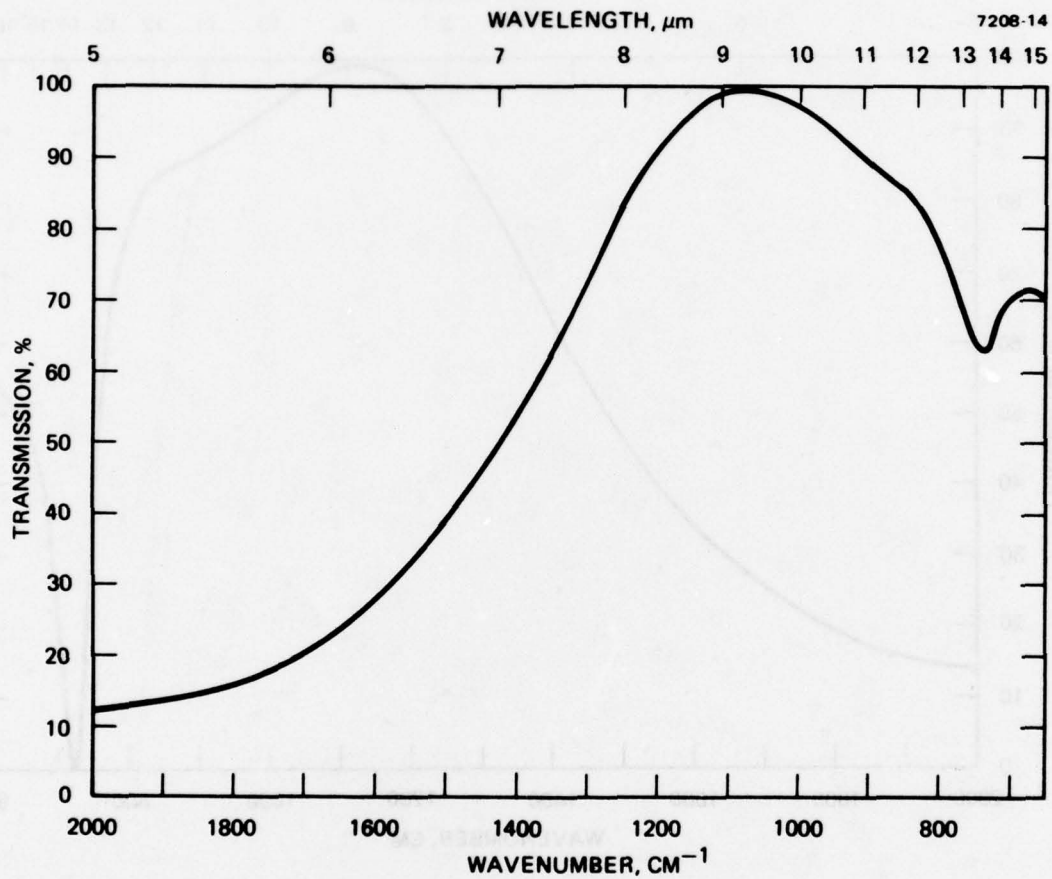


Figure 18. Transmission spectra of 150-4-14-7-4 ( $\text{As}_2\text{Se}_3/\text{NaF}/\text{As}_2\text{Se}_3$  AR coating), which exhibits 13.6  $\mu\text{m}$  absorption.

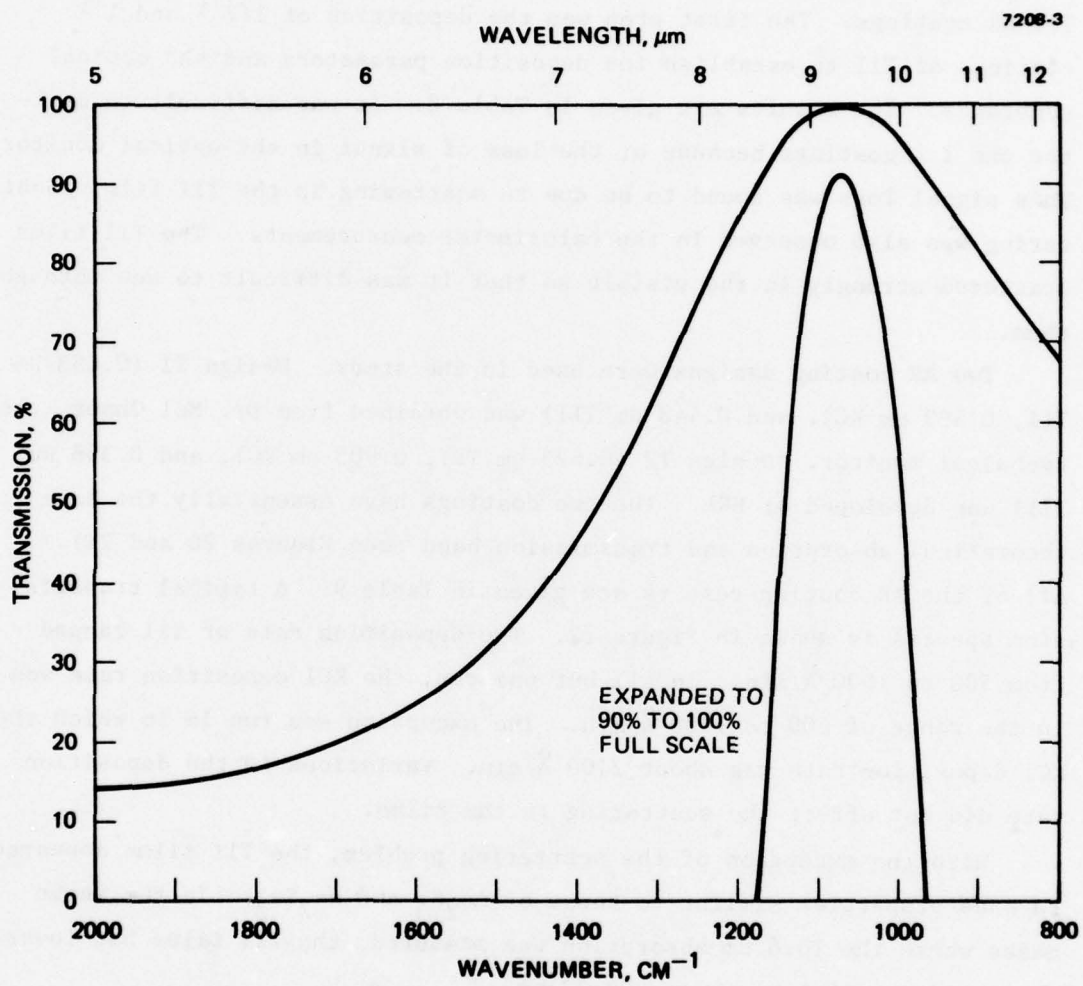


Figure 19. Transmission spectra of 174-5-30-9-1  
( $\text{As}_2\text{Se}_3/\text{NaF}/\text{As}_2\text{Se}_3$  AR coating).

#### E. TlI/KCl/TlI RESULTS

The last effort in the program was devoted to studying the TlI/KCl/TlI AR coatings. The first step was the deposition of  $1/2 \lambda$  and  $1 \lambda$  coatings of TlI to establish the deposition parameters and the optical constants. The results are given in Table 8. It was difficult to monitor the  $1 \lambda$  coatings because of the loss of signal in the optical monitor. This signal loss was found to be due to scattering in the TlI film. Scattering was also observed in the calorimeter measurements. The TlI films scattered strongly in the visible so that it was difficult to see through them.

Two AR coating designs were used in the study. Design T1 (0.853  $\mu\text{m}$  TlI, 0.599  $\mu\text{m}$  KCl, and 0.448  $\mu\text{m}$  TlI) was obtained from Dr. Mel Ohmer, the technical monitor. Design T2 (0.623  $\mu\text{m}$  TlI, 0.905  $\mu\text{m}$  KCl, and 0.358  $\mu\text{m}$  TlI) was developed at HRL. The two coatings have essentially the same theoretical absorption and transmission band (see Figures 20 and 21). All of the AR coating results are given in Table 9. A typical transmission spectra is shown in Figure 22. The deposition rate of TlI ranged from 500 to 1000  $\text{\AA}/\text{min}$ . In all but one run, the KCl deposition rate was in the range of 600 to 1200  $\text{\AA}/\text{min}$ . The exception was run 16 in which the KCl deposition rate was about 2100  $\text{\AA}/\text{min}$ . Variations in the deposition rate did not affect the scattering in the films.

With the exception of the scattering problem, the TlI films appeared to have properties similar to those of  $\text{As}_2\text{S}_3$  and  $\text{As}_2\text{Se}_3$ . In the seven cases where the 10.6  $\mu\text{m}$  absorption was measured, the TlI films had lower absorption at 10.6  $\mu\text{m}$  than at 9.27  $\mu\text{m}$ .

One run was made to determine the sensitivity of the TlI coatings to the vacuum environment. In run 16, the vacuum system (and thus the substrates) were not baked out. The total absorption of the sample and the coating absorption was significantly higher at both 9.27 and 10.6  $\mu\text{m}$  (see Table 10). This difference was in fact greater than that observed in a comparison of UHV- and non-UHV-deposited coatings performed under the DARPA program. There was no absorption band in the transmission spectrum of these samples as occurred in the  $\text{As}_2\text{Se}_3$  case. An example is shown in Figure 23.

Table 8. TII Film Data

Sample No.	Substrate Dopant	Coating Design	Transmission, Peak, $\mu\text{m}$	9.27 $\mu\text{m}$ Absorption Data <sup>a</sup>				Absorption Coefficient, $\text{cm}^{-1}$	
				Substrate, %	Sample, %	Coating, % per Surface			
1280A-12-1	Eu	$\frac{1}{2}\lambda$	9.17	0.15	0.31	0.16	8	1.93 $\mu\text{m}$ coating	
9-3A-12-2	Rb	$1\lambda$	9.31	0.11	0.68	0.57	1 4	3.91 $\mu\text{m}$ coating	
9-5A-12-3	Rb	$1\lambda$	10.14	0.10	0.68	0.58	1 4	4.26 $\mu\text{m}$ coating	
<sup>a</sup> Not measured at 10.6 $\mu\text{m}$									

6077

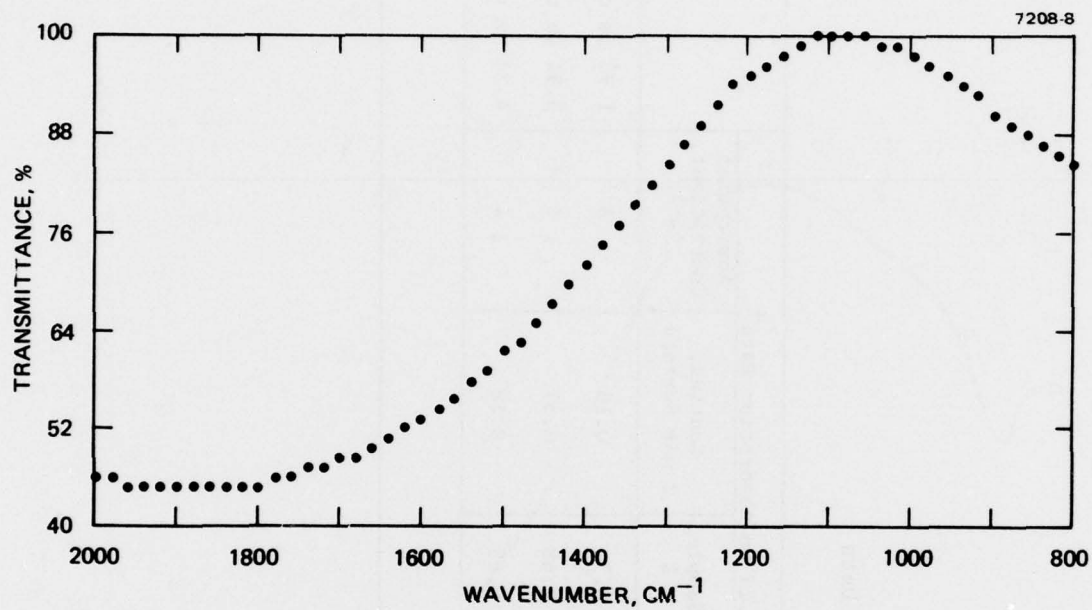


Figure 20. Theoretical transmission spectra of design T1.

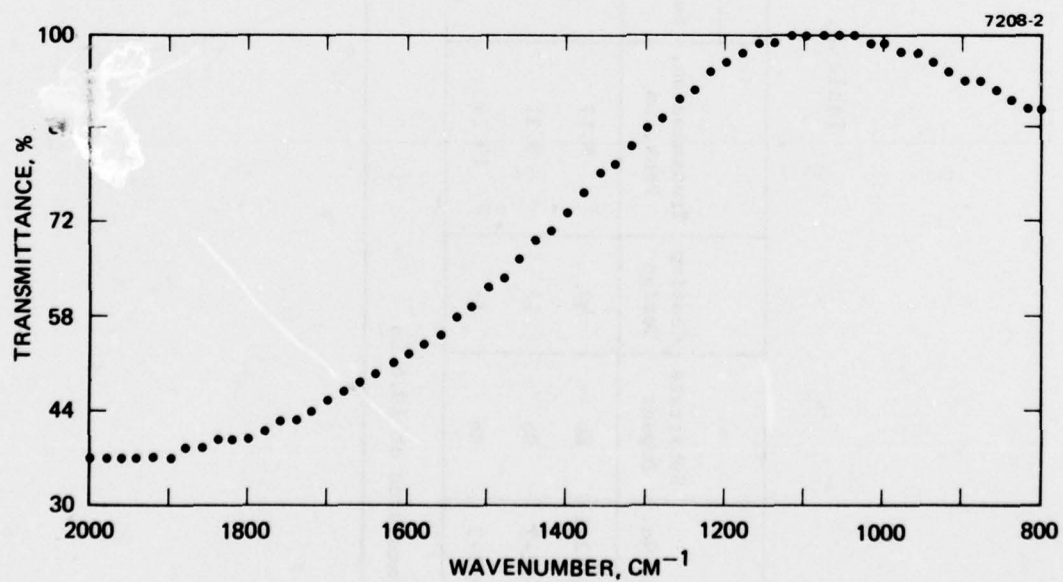


Figure 21. Theoretical transmission spectra of design T2.

Table 9. TlI/KCl/TlI AR Coating Data

Sample No.	Substrate Dopant	Coating Design	Transmission Peak, $\mu\text{m}$	Absorption Data						Remarks
				9.27 $\mu\text{m}$			10.6 $\mu\text{m}$			
				Substrate, %	Sample, %	Coating, % per Surface	Substrate, %	Sample, %	Coating, % per Surface	
8A6-12-4	Eu	T1	9.39	0.059	0.223	0.082	(a)	(a)		
9-16A-13-1	Rb	T1	9.90	0.24	(a)		(a)	(a)		Shutter jammed - heavy deposit
169-5-6A-13-2	Rb	T1	9.50	(a)	0.343	<0.17	(a)	(a)		Shutter leaking during deposition
8C4-13-3	Eu	T2	9.54	0.11	0.55	0.22	(a)	(a)		Shutter leaking during deposition
174-6-36A-13-4	Rb	T2	9.52	0.056	0.269	0.107	(a)	0.113	<0.056	
8F5-14-1	Rb	T1	9.9	0.100	0.266	0.083	(a)	0.166	<0.083	
8E2-14-2	Rb	T1	9.5	0.061	0.181	0.060	(a)	(a)		
8E3-14-3	Rb	T2	12.5	0.076	0.207	0.065	(a)	(a)		Over run TlI one side 1.048 $\mu\text{m}$ instead of 0.358 $\mu\text{m}$
886-14-4	Rb	T2	9.7	0.123	0.263	0.070	(a)	(a)		
12718-15-1	Eu	T2	9.35	0.272	0.213	<0.106	0.13	(a)		
8H6-15-2	Pb	T2	9.43	0.084	0.251	0.084	(a)	(a)		
8D14-15-3	Rb	T2	9.66	0.067	0.292	0.112	0.036	0.161	0.063	
8D13-15-4	Rb	T1	9.85	0.093	0.635	0.27	0.050	(a)		Small over run in KCl and TlI both sides
8D10-16-1	Rb	T1	9.66	0.064	0.725	0.33	(a)	(a)		Run 16 - system and samples not baked out: fast deposition rate for KCl; spots on surface
8E9-16-2	Rb	T1	9.5	0.115	0.761	0.32	(a)	0.292	<0.12	
8D5-16-3	Rb	T2	10.0	0.07	1.16	0.54	(a)	0.285	<0.14	
8D8-16-4	Rb	T2	9.88	0.07	0.39	0.41	(a)	0.422	<0.21	
1993-17-1	Rb	T2	9.66	1.03	0.67	<0.33	(a)	(a)		Unusually high absorption in substrate
1989-17-2	Rb	T2	9.57	0.072	0.304	0.116	(a)	(a)		
1994-17-3	Rb	T1	9.22	0.060	0.204	0.072	(a)	0.111	<0.055	
169-2-08-17-4	Rb	T1	9.26	0.110	0.397	0.143	(a)	(a)		
1990-18-1	Rb	T1	9.27	0.060	0.221	0.081	(a)	(a)		
1988-18-2	Rb	T1	9.33	0.063	0.214	0.075	(a)	(a)		
1991-18-3	Rb	T1	9.29	0.068	0.245	0.088	(a)	(a)		
1992-18-4	Rb	T1	9.17	0.074	0.210	0.068	(a)	(a)		

<sup>a</sup> Not measured.

<sup>a</sup>Not measured.

6077

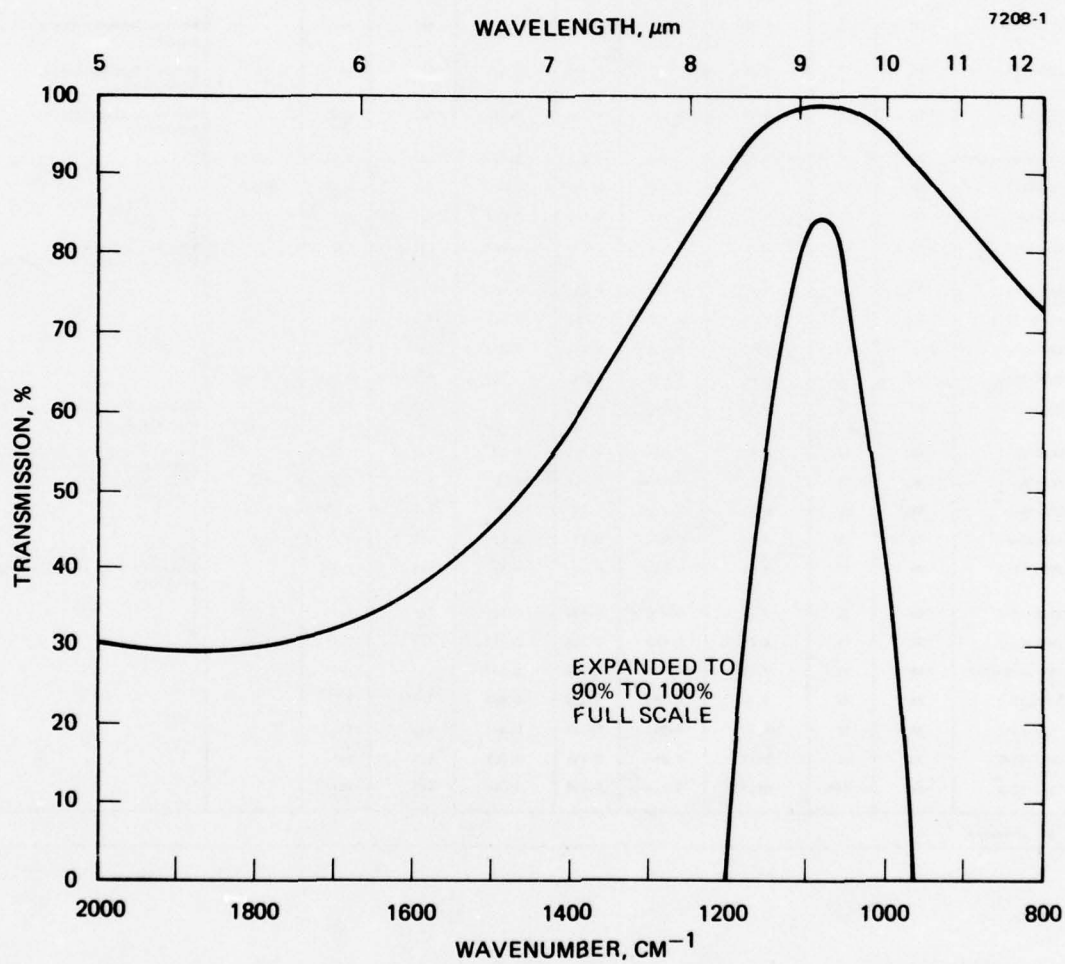


Figure 22. Transmission spectra of 1992-18-4 (TlI/KCl/TlI AR coating).

Table 10.

	9.27 $\mu\text{m}$		10.6 $\mu\text{m}$	
	Sample Absorption, %	Coating Absorption, % per Surface	Sample Absorption, %	Coating Absorption, % per Surface
UHV samples	0.223	0.082		
	0.269	0.107	0.113	<0.056
	0.266	0.083	0.166	<0.083
	0.181	0.060		
	0.207	0.065		
	0.263	0.070		
	0.213	<0.106		
	0.251	0.084		
	0.292	0.112	0.161	0.063
	0.304	0.116		
	0.204	0.072	0.111	<0.055
	0.397	0.143		
	0.221	0.081		
	0.214	0.075		
	0.245	0.088		
	0.210	0.068		
	<0.248 $\pm$ 0.052>	<0.087 $\pm$ 0.023>	<0.138 $\pm$ 0.030>	
Unbaked UHV samples	0.725	0.33		
	0.761	0.32	0.242	<0.12
	1.16	0.54	0.285	<0.14
	0.89	0.41	0.422	<0.21
	<0.88 $\pm$ 0.20>	<0.40 $\pm$ 0.10>	<0.316 $\pm$ 0.094>	

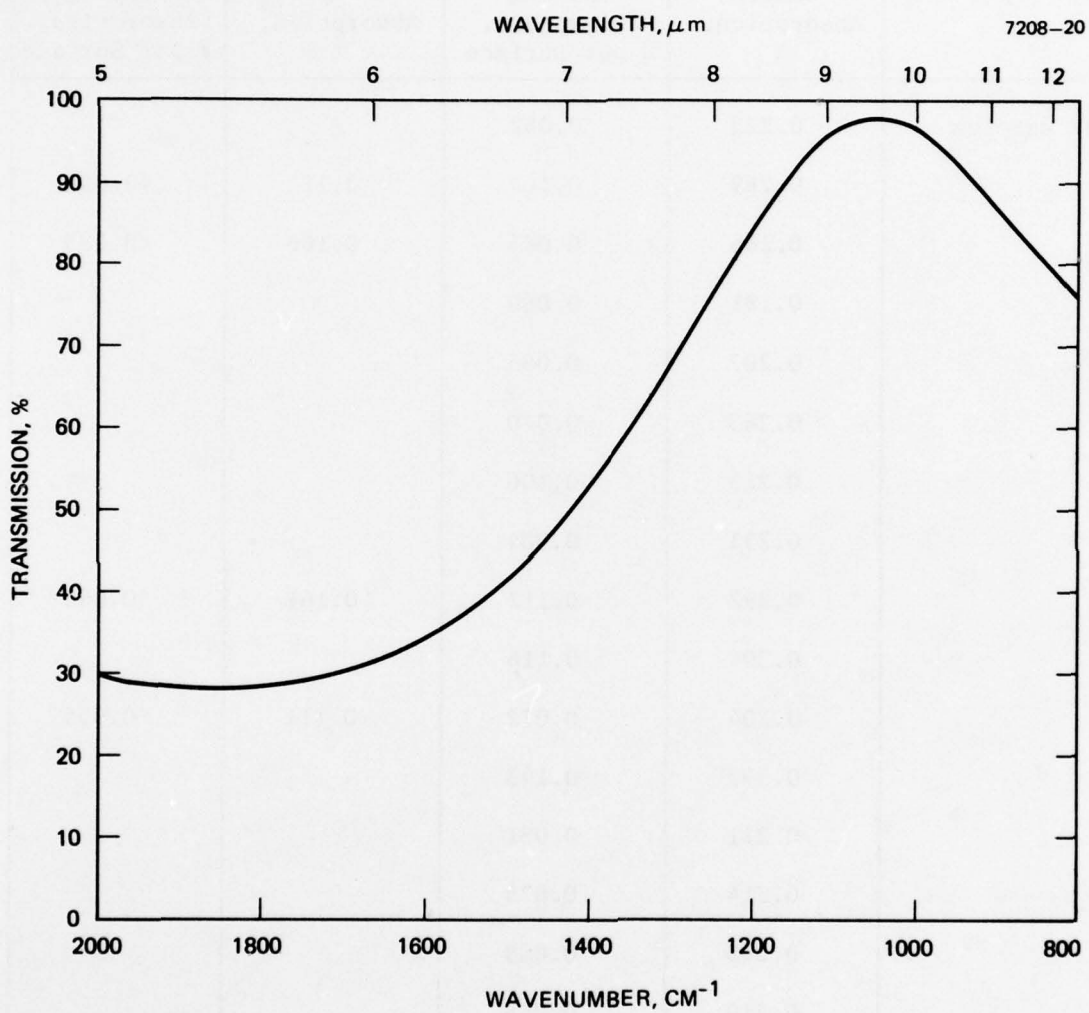


Figure 23. Transmission spectra of 8E9-16-2 (TlI/KCl/TlI AR coating).

The optical absorption of coatings produced from design T1 and T2 are essentially identical. Of the 16 successful UHV deposited samples, nine were of the T1 design and seven were of the T2 design. The mean value of the total absorption at  $9.27 \mu\text{m}$  was  $0.240 \pm 0.064\%$  for the T1 samples and  $0.257 \pm 0.037\%$  for the T2 samples. The coating absorption at  $9.27 \mu\text{m}$  was  $0.084 \pm 0.024\%$  per surface for the T1 samples and  $0.092 \pm 0.022\%$  per surface for the T2 samples. In each case the values lie within the standard deviations and thus must be considered indistinguishable.

There is a significant difference between these coatings produced under UHV conditions and similar coatings produced under conventional vacuum conditions. Design T1 is the same as design 5 described by Ohmer.<sup>7</sup> The mean value of the total absorption at  $9.27 \mu\text{m}$  of the five Ohmer samples of design 5 coating of TlI/KCl/TlI was  $0.34 \pm .07\%$ . This is significantly higher than the  $0.24 \pm 0.064\%$  value of the T1 samples.

#### F. POLYCRYSTALLINE KCl SUBSTRATE MATERIALS

Three types of stabilized polycrystalline KCl were used in this study. The initial studies were conducted with KCl doped with 1.75 mol% rubidium\* and with KCl doped with approximately 0.004 mol% europium.<sup>†</sup> The most pronounced difference between these materials was in their microstructure. The rubidium stabilized material had a more uniform distribution of crystallite sizes. They ranged from about 5 by 5  $\mu\text{m}$  to 10 by 30  $\mu\text{m}$  in size. The surface of the KCl appeared to have lines or columns that repeated at about 200 to 300  $\mu\text{m}$ . These lines consisted of areas that were mainly made of small crystallites. The area between the lines appeared to be composed of the large crystallites.

---

<sup>7</sup>M.C. Ohmer, "Thallium Iodide Coatings for Potassium Chloride for 9.27 microns," Report No. AFML-TR-77-157.

\*This material was purchased from the Ceramics Center of Honeywell, Inc. Golden Valley, Minn. 55422.

<sup>†</sup>This material was fabricated by the Honeywell Ceramics Center and furnished by the Air Force Materials Laboratory.

In the europium-doped KCl, the crystallite sizes had a much greater variation, ranging from 5 to 100  $\mu\text{m}$  in width. This material also had banded areas which consisted of regions of small and regions of large crystallites. These bands were about 1 to 2 mm apart. These bands appeared to run through the sample.

Both materials had areas in which grain growth (reversion to single crystal) had occurred. The rubidium-doped material appeared to be more sensitive to recrystallization. In some samples that had been coated and repolished, we observed that, after about 8 to 12 months, the material was essentially reconverted to large macrocrystals (about 1 cm in size). Only small areas of polycrystalline material remained.

Midway in the study, a second type of 1.75% rubidium stabilized polycrystalline KCl was put into use. It was forged at HRL from KCl that had been RAP-grown (at HRL). This material differs from the Honeywell material in two respects: (1) the HRL material is forged to about 70% reduction, versus 55% for the Honeywell material; and (2) the HRL material is made from RAP-grown KCl, and the Honeywell material is not.

The increased forging appears to disrupt the crystal to a greater degree. This disruption is reflected by the absence of the repeating patterns of microcrystals that were observed in the other two materials. Also, macrocrystals form much less frequently. They are limited to small regions of the sample and are found in a few of the samples.

#### G. COMPARISON OF 9.27 AND 10.6 $\mu\text{m}$ ABSORPTION IN KCl

Although this program was concerned with 9.27  $\mu\text{m}$  coatings and a companion program (DARPA funded) was concerned with 2 to 10.6  $\mu\text{m}$  coatings, we made every effort to measure the absorption of substrates used in these programs at both wavelengths whenever possible. A total of 72 substrates were characterized at both 9.27 and 10.6  $\mu\text{m}$ . The most interesting feature is that in only three cases (4% of the total) was the 9.27  $\mu\text{m}$  absorption lower than the 10.6  $\mu\text{m}$  value.

Table 11 summarizes the mean value of the 9.27/10.6  $\mu\text{m}$  absorption ratio for three types of polycrystalline KCl and for single crystal KCl.

Table 11. Comparison of 9.27/10.6  $\mu\text{m}$  Absorption in KCl

	Polycrystalline				Single Crystal (RAP Grown)
	Polycrystalline			Combined Polycrystalline	
	Honeywell Rb Doped	Honeywell Eu Doped	HRL (RAP) Rb Doped		
Samples measured at 9.27 and 10.6 $\mu\text{m}$					
No. of samples	11	8	19	38	34
Mean value of the 9.27/10.6 ratio	2.71 $\pm$ 1.19	2.28 $\pm$ 0.53	1.93 $\pm$ 0.93	2.23 $\pm$ 0.99	2.64 $\pm$ 1.25
Average of all 9.27 and 10.6 $\mu\text{m}$ measurements					
All 9.27 data No. of samples	38	20	27	85	37
Mean value of absorption x 10 <sup>3</sup> (cm <sup>-1</sup> )	1.54 $\pm$ 0.91	1.39 $\pm$ 0.72	1.00 $\pm$ 0.46	1.33 $\pm$ 0.78	0.79 $\pm$ 0.54
All 10.6 data	16	11	30	57	39
Mean value of absorption x 10 <sup>3</sup> (cm <sup>-1</sup> )	1.03 $\pm$ 1.20	0.86 $\pm$ 0.56	0.61 $\pm$ 0.40	0.78 $\pm$ 0.75	0.33 $\pm$ 0.19

6077

In view of the magnitude of the deviation in the mean values, we concluded that the 9.27  $\mu\text{m}$  value is about 2.5 times greater than the 10.6  $\mu\text{m}$  value.

In addition to the paired measurements, we have included all of the absorption values obtained in these two programs. If we make the approximation that the average sample thickness and the distribution in thickness is the same in each group, it is possible to compare the values. The highest absorption was observed in the Honeywell 1.75% Rb-doped polycrystalline KCl, followed by the 0.004% Eu-doped KCl, and the HRL 1.75% doped polycrystalline KCl. The lowest values were obtained in the single crystal KCl. Similar results were observed in a comparison of the absorption in coated samples. Two conclusions can be drawn from this:

- The RAP-grown KCl has a lower absorption than does the normal KCl.
- The Honeywell 1.75% Rb-doped material has a higher absorption than does the 0.004% Eu-doped KCl or the HRL 1.75% Rb-doped KCl.

#### H. RECRYSTALLIZATION IN POLYCRYSTALLINE KCl

Polycrystalline KCl substrates that had been coated and tested in previous studies were supplied by AFML to HRL for use in the TII coating study. The samples were polished to remove the coatings. After the coatings were removed, we observed internal cleavage or fracture planes in 7 of the 15 samples. The fractured samples were examined and were found to have reverted from polycrystalline to large macrocrystals over most of the sample. The fracture planes appeared to be located at the edges or within the macrocrystals.

An analysis of all the samples was made. We found all the rubidium-doped material had reverted to macrocrystalline, while the two europium-doped KCl remained fine grain polycrystalline. An analysis of the sample histories indicated that the samples with fracture planes were those that had been subjected to environmental tests. The data is summarized in Table 12.

Table 12. History of Doped Polycrystalline Samples

Honeywell No.	AFM No.	Dopant	Prior Tests	As Received Condition	Condition after Polishing	Extent of Macro-Crystal Growth
8A6	1392	Eu				All poly
8C4	1478	Eu				All poly
8B5	1481	Rb			Cleavage	
8B6	1393	Rb				All macro
8D15	2064	Rb	Adhesion		Cleavage	3/4 macro
8E2	2050	Rb				All macro
8E3	2051	Rb				All macro
8E9	1844	Rb				
8F2	2067	Rb	Abrasion, Adhesion		Cleavage	
8F5	2055	Rb				
8G3	2069	Rb	Abrasion, dhesion	Internal haze	Internal cleavage	2/3 macro
8H1	2073	Rb	UV		Cleavage	2/3 macro
8H2	2074	Rb	Adhesion		Cleavage	
8H6	2056	Rb				All macro
8H7	2057	Rb	Laser damage		Laser damage spots	

6077

I. EFFECTS OF ETCHING ON SURFACE FLATNESS

Etching of mechanically polished KCl is essential to stabilize the surface (i.e., prevent fogging by atmospheric moisture) and to remove from the surface the damaged material that results from the polishing process. Studies have shown that the etch rate is highest at first and that it falls rapidly. The highest rate is associated with the solution of the maximum damage region of the KCl.

In this work, we limited the process to a 15 sec etch in concentrated HCl. This represents a minimum exposure that removed the major damaged material. A limited number of samples were re-etched, and the absorption measurements did not show any significant change. Microscopic examination of the surface after the 15 sec etch failed to show any pronounced faceting.

Surface flatness was measured before and after etching on six samples. The changes in flatness were less than  $2\lambda$ . This is summarized in Table 13. The flatness was measured with a Davidson interferometer with 5770 Å light.

Table 13. Changes in Surface Flatness after a 15 s Etch

Sample	Before		After	
	Side 1	Side 2	Side 1	Side 2
8B6	$1/2\lambda$	$1/2\lambda$	$2\lambda$	$1\lambda$
8E2	$1/8\lambda$	$1/2\lambda$	$1\lambda$	$1-1/2\lambda$
8E3	$1/4\lambda$	$1/2\lambda$	$1\lambda$	$2\lambda$
8F5	$1/2\lambda$	$1/4\lambda$	$1\lambda$	$2\lambda$
8H6	$1/4\lambda$	$2\lambda$	$2\lambda$	$5\lambda$

6077

#### J. ENVIRONMENTAL TESTS

Three samples of the TlI/KCl/TlI AR coating were subjected to environmental tests. The results are summarized in Table 14.

Table 14. Results of Environmental Tests

Sample	Abrasion Test (MIL-C-675A (20-Rub Eraser)	Adherence Test MIL-M-13508B (Scotch Tape)	Humidity Test MIL-C-675A (24 hours)
9-16A-13-1	Failed	Failed	Failed
8C4-13-3	Failed	Passed	Failed
169-5-6A-13-2	Failed	Passed	Failed

6077

#### K. LASER DAMAGE TEST RESULTS

The first coatings tested were ZnSe/KCl/ZnSe AR coatings. These films exhibit a tendency to craze after several months, which may be reflected in the damage results shown in Table 15. Included in this summary are some UHV and non-UHV samples produced under a DARPA program. These results were included for completeness.

Since the damage level is variable in the focused beam tests, we present the power level at which damage first was observed and the maximum power level at which there was at least 50% survival.

The largest group of samples tested were AR coatings of  $\text{As}_2\text{Se}_3/\text{KCl}/\text{As}_2\text{Se}_3$ . The first group (9-8-6-1, 8-3-6-3, and 9-11-6-2) had a very high 9.27  $\mu\text{m}$  absorption and a 9  $\mu\text{m}$  absorption band, which indicated the presence of oxide impurity in the  $\text{As}_2\text{Se}_3$  films. This group had a low damage threshold. The second group (129-1-49-1, 129-2-49-2, 155-5-12-24-10-2, and 64-25-10-3), which had much lower 9.27  $\mu\text{m}$  absorption, were undamaged at 10.6  $\mu\text{m}$  and damaged at the maximum level at 9.27  $\mu\text{m}$ . The third group (78-13, 70-3, and 78-5) were non-UHV samples that had significantly larger absorption at 9.27 and 10.6  $\mu\text{m}$ . Two samples were damaged at low levels and one was undamaged at the maximum level. Two single

Table 15. Results of Laser Damage Studies

Coating	Sample No.	Coating Absorption (% Per Surface)		Power Level, kW/cm <sup>2</sup>				Remarks
		9.27 μm	10.6 μm	Focused Minimum Damage	10.6 μm Maximum No Damage	Broad Beam		
						10.6 μm	9.27 μm	
As <sub>2</sub> Se <sub>3</sub> /KCl/As <sub>2</sub> Se <sub>3</sub>	9-8-6-1	0.35	<0.054	32 <sup>a</sup>	108			Significant 9 μm absorption band
	8-3-6-3	0.36	0.048	49 <sup>a</sup>	108			Significant 9 μm absorption band
	9-11-6-2	0.32	<0.040				2.6	Significant 9 μm absorption band
	129-1-49-1	<0.047	0.026			>7.5		
	129-2-49-2	0.039	0.068				7.5	
	155-5-12-24-10-2	0.090	0.017			>7.5		
	64-25-10-3	0.105	0.033			>7.5		
	78-13	0.37	0.43			5.3		Non-UHV sample-DARPA
	70-3	0.15	0.21				3.5	Non-UHV sample-DARPA
1λ As <sub>2</sub> Se <sub>3</sub>	78-5	0.20	0.14			>7.5		Non-UHV sample-DARPA
	150-4-15-7-3	0.13	0.016			>7.5		
As <sub>2</sub> S <sub>3</sub> /KCl/As <sub>2</sub> S <sub>3</sub>	174-5-29-9-4	0.045	0.028				3.5	
	82-8	b	b	109	109			Non-UHV sample-DARPA-1 yr old
1/2λ As <sub>2</sub> S <sub>3</sub>	63-11	0.23	0.072	>109	109	>7.5		Non-UHV sample-DARPA
	152-3-46-2	b	0.25	>109	109			
	8-1-5-3	0.19	b	>109	109		>7.5	
As <sub>2</sub> Se <sub>3</sub> /NaF/As <sub>2</sub> Se <sub>3</sub>	8-4-5-2	0.14	b			>7.5		
	174-5-30-9-1	0.033	0.16			1.8		
	174-8-33-9-2	0.079	0.27				4.5	
ZnSe/KCl/ZnSe	1274-2-3	0.15	b	14	109			
	1277-2-2	0.03	b	32	109			
	9-15-4-2	<0.22	b	32	109			
	109-RF4	b	0.30	30	78			2.5 cm diameter UHV sample - DARPA-8 months old
	109-RF5	b	0.20	108	109			2.5 cm diameter UHV sample - DARPA-8 months old
	146-10	b	0.26	42	86			2.5 cm diameter UHV sample - DARPA-8 months old
	67-B3	b	0.05	20	108			2.5 cm diameter UHV sample - DARPA-1 yr old
ZnSe/ThF <sub>4</sub> /ZnSe	129-8	b	0.04	20	108			2.5 cm diameter UHV sample - DARPA-1 yr old
	95-B2	b	0.07	32	108			2.5 cm diameter UHV sample - DARPA-1 yr old
	67-A3	b	0.20	20	39			2.5 cm diameter UHV sample - DARPA-1 yr old
	82-6	b	b	45 <sup>a</sup>	109			Non-UHV sample - DARPA

<sup>a</sup>Films cleanly ablated - no substrate damage.  
<sup>b</sup>Not measured.

<sup>a</sup>Films cleanly ablated - no substrate damage.<sup>b</sup>Not measured.

6077

layer films of  $\text{As}_2\text{Se}_3$  were tested. One was undamaged at  $10.6\text{ }\mu\text{m}$  and the other failed at  $3.5\text{ kW/cm}^2$  at  $9.27\text{ }\mu\text{m}$ . Although there are fewer  $\text{As}_2\text{S}_3$  samples, these coatings exhibited a much higher damage resistance. Of three samples of AR coatings of  $\text{As}_2\text{S}_3/\text{KCl}/\text{As}_2\text{S}_3$ , No. 82-8 was damaged at only one point at the highest power level, No. 63-11 was undamaged in both the focused and broad beam  $9.27\text{ }\mu\text{m}$  tests. The three samples of single-layer  $\text{As}_2\text{S}_3$  films were undamaged at all tests.

The two samples of films containing NaF had high  $10.6\text{ }\mu\text{m}$  absorption. These samples exhibited low damage threshold. In general, the films containing ZnSe exhibited a few sites that were damaged at low power level and a larger number of sites that could not be damaged at the highest power levels.

Although the number of samples and tests are not sufficient to establish precise values of laser damage threshold, it is possible to infer the following conclusions. The  $\text{As}_2\text{S}_3$ , which is less sensitive than  $\text{As}_2\text{Se}_3$  to the vacuum environment during deposition, has the highest damage threshold ( $7.5\text{ kW/cm}^2$  broad beam and  $109\text{ kW/cm}^2$  focused) of the materials tested. The  $\text{As}_2\text{Se}_3$  films that were deposited under UHV conditions and were oxide free also had a similar damage threshold.

#### L. ENVIRONMENTAL CONSEQUENCES

Some optical films used in this program (such as  $\text{ThF}_4$ , ZnSe,  $\text{As}_2\text{S}_3$ ,  $\text{PbF}_2$ , etc.) may have potential environmental hazards when these programs reach manufacturing scale-up and production; for example:

1.  $\text{ThF}_4$  has some radioactivity (although it is a weak alpha emitter and does not pose a great hazard because of this radioactivity) and it is a heavy metal compound. Adequate precaution should be taken to prevent inhalation of  $\text{ThF}_4$  particulate material. It is suggested that at a minimum of twice a year a radiation count should be taken over the operating environment where such films are produced to ensure good housekeeping and a safe radioactive environment.
2. Selenium and arsenic compounds are known to be toxic and provisions should be made in any manufacturing scale-up environment to have adequate ventilation and scrubbing facilities installed to prevent any selenium or arsenic vapor escaping into the local environment. At a minimum of twice a year, personnel should be examined for heavy metals ingestion.

#### M. INDEX OF REFRACTION

The refractive index of  $\text{As}_2\text{S}_3$ ,  $\text{As}_2\text{Se}_3$ , and TlI were measured during this study. Single-layer coatings were deposited on KCl. A mask was used to obtain a sharp edge to the deposit. The film thickness was determined with a Carl Zeiss interference microscope. We attempted to use a Sloan Dektak, but found it to be insensitive and not reproducible. The maximum and minimum points in transmission were determined from transmission spectra taken in a Beckman IR-12 spectrophotometer. The refractive index at  $9.24\text{ }\mu\text{m}$  was determined to be  $2.80 \pm 0.03$  for  $\text{As}_2\text{Se}_3$ ,  $2.36 \pm 0.03$  for  $\text{As}_2\text{S}_3$ , and  $2.38 \pm 0.03$  for TlI at  $9.27\text{ }\mu\text{m}$ .

## SECTION IV

### SUMMARY

Five 9.27  $\mu\text{m}$  AR coatings for polycrystalline KCl were developed in this study. These coatings achieved low optical absorption losses by deposition under UHV conditions. The three layer coatings of ZnSe/KCl/ZnSe,  $\text{As}_2\text{S}_3/\text{KCl}/\text{As}_2\text{S}_3$ ,  $\text{As}_2\text{Se}_3/\text{KCl}/\text{As}_2\text{Se}_3$ ,  $\text{As}_2\text{Se}_3/\text{NaF}/\text{As}_2\text{Se}_3$ , and TlI/KCl/TlI had absorption losses of 0.03 to 0.09% per surface. The results are summarized in Table 16. These values are significantly lower than the values obtained from coatings produced under conventional vacuum conditions.

AR coatings of  $\text{As}_2\text{S}_3/\text{KCl}/\text{As}_2\text{S}_3$  were undamaged by exposure to 10.6  $\mu\text{m}$  cw laser radiation at power levels of 7.5  $\text{kW}/\text{cm}^2$  for the broad beam exposure and 109  $\text{kW}/\text{cm}^2$  for the focused beam. Similar  $\text{As}_2\text{Se}_3/\text{KCl}/\text{As}_2\text{Se}_3$  films deposited under UHV conditions exhibited similar behavior.

As in previous studies, the vacuum conditions present during the deposition were found to be critical to the coating absorption. Both  $\text{As}_2\text{Se}_3$  and TlI films had significantly higher absorption when the films were deposited in the presence of water vapor at about  $1 \times 10^{-8}$  Torr partial pressure than did films deposited under water vapor of less than  $1 \times 10^{-10}$  Torr partial pressure.

A polishing technique was developed to fabricate in a reproducible manner KCl surfaces that have low optical absorption and good flatness and parallelism. A 15 s etch in concentrated HCl was found to be adequate to remove surface damage and stabilize the surface without decreasing the flatness by more than  $2 \lambda$ .

A technique was developed for deposition of coatings on both surfaces of a KCl substrate during a single evacuation. Efficient evaporation sources were developed. A stabilized interferometric-optical technique for accurate monitoring of the film thickness during deposition was developed.

A mass spectrometer was used to analyze the gases present during film deposition to identify any impurities present in the film materials. Techniques for preparation of pure materials were developed. Also a RAP technique was used for cleaning impure materials.

Rubidium-doped polycrystalline KCl (produced by 55% reduction of the KCl ingot) was observed to revert to macrocrystalline material,

while europium-doped polycrystalline KCl remained polycrystalline. Also the Rb-doped KCl had a higher absorption than did the Eu-doped KCl. The lowest absorption was observed in Rb-doped RAP-grown KCl forged to a 70% reduction.

Table 16. Summary of Lowest Values  
Coating Absorption at 9.27  $\mu\text{m}$

AR Coating Design	Theoretical Value, % Per Surface	Observed Value, % Per Surface
ZnSe/KCl/ZnSe	0.016	0.031
As <sub>2</sub> S <sub>3</sub> /KCl/As <sub>2</sub> S <sub>3</sub>	0.024	0.069
As <sub>2</sub> Se <sub>3</sub> /KCl/As <sub>2</sub> Se <sub>3</sub>	0.020	0.090 <sup>a</sup>
As <sub>2</sub> Se <sub>3</sub> /NaF/As <sub>2</sub> Se <sub>3</sub>	0.019	0.033
TlI/KCl/TlI	0.024	0.060
<sup>a</sup> Obtained a 0.019% value in a DARPA sample.		

6077

## APPENDIX A

### MATERIALS FOR 9.27 $\mu$ m AR COATINGS

A comprehensive literature search was conducted to establish a list of materials with the best potential for producing low-loss 9.27  $\mu$ m AR coatings. One objective was to discover new materials that could be used. Another goal was to obtain a complete set of physical and optical parameters for the materials. The most important parameters include the bulk and thin-film absorption constant, the refractive index, the water solubility, and the linear expansion coefficient.

The first step was to compile the information available in the standard reference (Refs. 1-11). The search was extended to the Physical Abstracts for the period 1960 through 1 June 1976. The topics searched included light absorption, optical films, optical materials, and specific chemicals. Also a similar search was made of the EPIC Guide to the Literature, volumes 1, 2, and 3.

The search produced a list of 145 materials that had been cited in the literature. Of these, 102 (listed in Table A-1) were dropped from consideration either because there was insufficient information or because the material was not suitable for use in 9.27  $\mu$ m coatings. The remaining 43 materials (listed in Table A-2) were considered in greater detail. A search was made in the Chemical Abstracts for citations about these specific compounds.

Nine materials were selected, and these are listed in Table A-3. Because of the limited amount of information about TlI, we have included KRS-5 in Table A-3. This material is a mixture of TlBr and TlI. It should provide a guide to the properties of TlI. The values presented in Table A-3 are the most recent ones obtained from the cited references and Ref. 12-13.

Table A-1

AlSb	CaO	PbSe	Se
AlN	Ce <sub>2</sub> O <sub>3</sub>	PbS	Si <sub>3</sub> N <sub>4</sub>
AlP	Ce <sub>2</sub> S <sub>3</sub>	LiBr	Si <sub>2</sub> O <sub>3</sub>
Sb <sub>2</sub> S <sub>3</sub>	CsBr	LiCl	AgBr
As <sub>2</sub> S <sub>5</sub>	CsCl	LiI	Ag <sub>2</sub> S
As <sub>2</sub> O <sub>3</sub>	CsI	Li <sub>2</sub> O	Ag <sub>2</sub> S <sub>3</sub>
As <sub>2</sub> Se <sub>5</sub>	Cs <sub>2</sub> O <sub>3</sub>	MnO	Ag <sub>3</sub> AsS <sub>3</sub>
As <sub>2</sub> Te <sub>3</sub>	CoO	HgO	NaBr
As <sub>2</sub> Te <sub>5</sub>	CuBr	HgSe	NaI
AlAs	CuCl	HgS	Na <sub>2</sub> O
BaBr <sub>2</sub>	Cu <sub>2</sub> O	HgTe	SrO
BaO	Cr <sub>2</sub> O <sub>3</sub>	MoO <sub>3</sub>	SrS
BaSe	Gd <sub>2</sub> O <sub>3</sub>	MoS <sub>2</sub>	Ta <sub>2</sub> O <sub>5</sub>
BaS	Ga <sub>2</sub> O <sub>3</sub>	NiO	Te
BaTe	GeO <sub>2</sub>	KF	TlBr
Bi <sub>2</sub> O <sub>3</sub>	GeTe	KI	TlCl
Bi <sub>2</sub> Se <sub>3</sub>	HfO <sub>2</sub>	K <sub>2</sub> O	TlS <sub>2</sub>
Bi <sub>2</sub> Te <sub>3</sub>	InSb	Pr <sub>2</sub> O <sub>3</sub>	SnO <sub>2</sub>
B <sub>2</sub> O <sub>3</sub>	InAs	RbBr	SnTe
BaTiO <sub>2</sub>	In <sub>2</sub> O <sub>3</sub>	RbCl	TiO <sub>2</sub>
Cd <sub>3</sub> As <sub>2</sub>	InP	RbF	WO <sub>3</sub>
CdCl <sub>2</sub>	Fe <sub>2</sub> O <sub>3</sub>	RbI	V <sub>2</sub> O <sub>5</sub>
CdF <sub>2</sub>	LaF <sub>3</sub>	Rb <sub>2</sub> O	ZnBr <sub>2</sub>
CdO	PbBr <sub>2</sub>	Sm <sub>2</sub> O <sub>3</sub>	ZnO
CaAl <sub>2</sub> O <sub>4</sub>	PbCl <sub>2</sub>	Sc <sub>2</sub> O <sub>3</sub>	ZnTe
CaCO <sub>3</sub>	PbO		

6077

Table A-2.

$\text{Al}_2\text{O}_3$	GaAs	Si
$\text{Sb}_2\text{O}_3$	Ge	SiO
$\text{As}_2\text{Se}_3$	GeS	AgCl
$\text{As}_2\text{S}_3$	GeSe	NaCl
$\text{BaF}_2$	$\text{HfF}_4$	NaF
$\text{BiF}_3$	$\text{PbF}_2$	$\text{SrF}_2$
CdSe	PbTe	$\text{SrTiO}_3$
CdS	LiF	TlI
CdTe	$\text{MgF}_2$	$\text{ThF}_4$
$\text{CaF}_2$	MgO	$\text{YbF}_3$
C	KBr	$\text{Y}_2\text{O}_3$
$\text{CeF}_3$	KCl	Yttralox ( $\text{Y}_2\text{O}_3 + \text{ThO}_2$ )
$\text{CeO}_2$	$\text{KGaF}_4$	ZnSe
$\text{CoF}_2$	$\text{PrF}_3$	ZnS
		$\text{ZrO}_2$

6077

#### APPENDIX A REFERENCES

1. C. S. Sahagian and C. A. Pitka, "Compendium on High Power IR Laser Window Materials," (LQ-10 Program), AFCRL-75-0170 (1972).
2. S. K. Dickinson, "IR Laser Window Material Property Data for ZnSe, KCl, NaCl, CaF<sub>2</sub>, S<sub>r</sub>F<sub>2</sub>, and BrF<sub>2</sub>," AFCRL-TR-65-0318 (1975).
3. W. L. Wolfe, "Handbook of Military IR Technology," Office of Naval Research, Dept. of Navy (1965).
4. A. J. Moses, "Refractive Index of Optical Materials in the Infrared Region," Hughes Aircraft Co., Jan. 1970.
5. A. J. Moses, "Optical Materials Properties," Handbook of Electronic Materials (IFI Plenum, 1971).
6. S. S. Ballard, K. A. McCarthy, and W. L. Wolfe, "Optical Materials for IR Instrumentation," University of Michigan (1958). AD 217 367 and its supplement AD 255699.
7. J. A. Jamieson et al., Infrared Physics and Engineering (McGraw Hill, 1963).
8. P. W. Kruse, L. D. McGlaughlin, and R. B. McQuistan, Elements of Infrared Technology (John Wiley, 1962).
9. "Compendium of Laser Window Materials Properties," University of Dayton Research Inst., Contract F 29601-75-C-0031, AD 80339, Feb. 1976.
10. M. Sparks, "Theoretical Studies of Materials for High Power Infrared Coatings," sixth Tech. Report, Contract DAHC 15-73-C-0127, 31 Dec. 1975.
11. Handbook of Chemistry and Physics, 54th. ed., CRC Press (1973).
12. H.Y.B. Mar and E. Bernal, J. Vac. Sci. Technol. 12, 919 (1975).
13. W. Heitmann and E. Ritter, Appl. Opt. 7, 307 (1968).

PRECEDING PAGE BLANK-NOT FILMED

## APPENDIX B

### SUMMARY OF SURFACE PREPARATION TECHNIQUES

#### SURFACE PREPARATION

7208-16

- SUBSTRATES HANDGROUND ON SiC PAPER TO UNIFORM THICKNESS
- SAMPLES ATTACHED TO GLASS MANDREL WITH WAX
- GROUND ON A CAST IRON LAP WITH LOOSE GRIT 20  $\mu\text{m}$   $\text{Al}_2\text{O}_3$  AND ETHYLENE GLYCOL TO REMOVE AT LEAST 0.1 MM OF KCl
- GROUND ON A GLASS LAP WITH LOOSE GRIT 9  $\mu\text{m}$   $\text{Al}_2\text{O}_3$  AND ETHYLENE GLYCOL TO REMOVE AT LEAST 0.05 MM OF KCl
- ETCHED IN CONCENTRATED HCl FOR 3 MIN
- POLISHED ON A SWISS PITCH LAP WITH LINDE A AND PROPANEDIOL FOR AT LEAST 4 HOURS
- ULTRASONIC CLEANING IN XYLENE
- REVERSE SIDE FINISHED
- LIGHT BUFF ON POLYTEX SUPREME WITH LINDE B AND ISOPROPYL ALCOHOL
- ETCHED IN CONCENTRATED HCl FOR 15 SEC
- RINSED WITH ISOPROPYL ALCOHOL
- DRIED IN A  $\text{N}_2$  GAS STREAM

PRECEDING PAGE BLANK-NOT FILMED